UNITED STATES
DEPARTMENT OF THE INTERIOR
BUREAU OF RECLAMATION

- - -

HYDRAULIC LABORATORY REPORT NO. 97

- - -

EXPERIMENTAL DETERMINATION OF DESIGN DATA FOR DESIGN OF JET PUMPS FOR BOULDER DAM POWER PLANT

By

H. M. MARTIN
S. E. RICE

- - -

Denver, Colorado
June 1941

HYD 97

UNITED STATES
DEPARTMENT OF THE INTERIOR
BUREAU OF RECLAMATION

Branch of Design and Construction
Engineering and Geological Control
and Research Division
Denver, Colorado
July 19, 1945

Laboratory Report No. 97
Hydraulic Laboratory
Compiled by: H. M. Martin
S. E. Rice
Reviewed by: G. J. Hornsby

Subject: The experimental determination of design data for the design of jet pumps for the Boulder power plant (HM-15).

I. SYNOPSIS

In the design of jet pumps for the circulation of cooling water for generators and transformers and for other pumping purposes at Boulder Dam powerhouse, it was necessary to determine the degree of momentum transfer or apparent shear between the water jets. For this purpose a series of tests was made with two concentric circular jets discharging vertically downward into the atmosphere.

The apparent shear was determined from the following data obtained experimentally; the discharge of each of the nozzles, the shape of the mixing jets, the length required for mixing, the boundary between the jets, and the velocity distribution throughout the mixing jets.

In the course of these tests it was thought that the mixing length of the jets could be reduced or a greater or quicker exchange of momentum between the jets could be attained by the change in shape of the driving nozzle. To determine the shape of the driving nozzle which caused the greatest transfer of momentum, nozzles of various designs were tested with the same entraining nozzle. It was found that only one nozzle had a greater pumping efficiency than the conventional circular nozzle; this was an eight-legged star-shaped nozzle. The transfer of momentum from its high velocity jet was greater than from the circular jet but the coefficient of discharge from the circular nozzle was greater. All other nozzles tested were inferior to the circular nozzle with regard to the degree of transfer of momentum and the coefficient of discharge.

II. INTRODUCTION

General. At Boulder Dam powerhouse, water-jet pumps such as illustrated in figure 1 are used for pumping purposes and to supply cooling water. In high head plants it is more economical to pump tail water with headwater (in a jet pump) and use the combined discharge for cooling than to throttle headwater or install additional turbine capacity and tail-water pumps. At Boulder Dam, station-service power is limited. Therefore, jet pumps are particularly feasible for pumping cooling water and for general pumping purposes at Boulder Dam.

The principle of operation of all jet pumps is, in general, the same; the driving jets are formed in nozzles which convert the pressure energy into velocity. The high-speed particles of the driving jet then mix with the slower moving particles of the material to be pumped. There is an exchange of momentum and the driving and driven streams approach the same velocity. If this takes place at constant pressure without wall friction, the momentum lost by one jet is gained by the other. The energy lost by one stream is partly but never fully recovered by the other stream. Most jet pumps include a diffuser in which the velocity energy of the mised jets is partially reconverted into pressure energy.

Water-jet pumps are most efficient when the quantities of suction and driving water are of the same order of magnitude. For certain applications, however, efficiency is not the important consideration. As an illustration, the jet pump can be used with large-quantity ratios as an energy-absorbing device for pressure reduction.

Jet pumps have been manufactured and used for many years. Theory of jet apparatus is yet in an undeveloped stage and experimentation constitutes a very important part in the construction of jet apparatus. As the jet pumps to be designed for the Boulder powerhouse were relatively large and operated under a particularly high head, it was necessary to determine the degree of momentum transfer or apparent shear between the jets to be able to design the mixing-chamber length correctly. These data were needed to design the mixing chamber to prevent cavitation and to insure that mixing of the jets is complete before they enter the diffuser.

To determine the value of the momentum transfer between the water jets, a series of tests was made with two concentric jets discharging into the atmosphere. Two concentric circular nozzles were set in the bottom of a tank, the inner nozzle discharging with a high velocity and the outer nozzle discharging with a low velocity under a relatively low head.

To simplify the analysis of the data, the nozzles were made to discharge vertically downward into the atmosphere, the mixing pressure, therefore, remaining constant. In this manner, the wall friction around the outer jet, as actually exists in the jet pump, was eliminated. The friction between the smooth jet and the air is negligibly small.

The data needed for the determination of the apparent shear factor between the high- and low-velocity jets were; the discharge of each of the nozzles, the shape of the mixing jets, the length required for mixing, the boundary between the jets, and the velocity distribution throughout the mixing jets.

III. DETERMINATION OF DEGREE OF MOMENTUM TRANSFER OR APPARENT SHEAR BETWEEN WATER JETS

Laboratory equipment and testing procedure. Two concentric nozzles were installed in the bottom of a steel tank as shown in figure 2. The discharge of the outer nozzle was maintained by a centrifugal pump and measured by a 90-degree V-notch weir which discharged into the nozzle head tank. The discharge of the inner nozzle was maintained by the same pump and was measured by inserting a piezometer at its base and calibrating for various pressures. It was controlled by a gate valve.

A profilometer, a general view of which is shown on plate I, was suspended from the bottom of the head tank and as nearly concentric with the nozzles as practicable. As four diameters of the jet were measures, absolute concentricity of the profilometer about the nozzles was not necessary as the jet surface was measured with a chisel point approximately 3/16 inch wide. Slight eccentricity of

the profilometer did not affect the accuracy of the diameter measurements. The water-surface-point gage measurements were read to thousandths of an inch.

Velocity traverses were made with a pitot tube having only a dynamic pressure leg. As the jets were discharging into the atmosphere, the velocity head was read directly.

It was necessary to install baffles and radial guide vanes to remove the swirls and eddies in the outer nozzle head tank. Surface floats eliminated the most serious vortices.

It was found that the jet from the outer nozzle was the smoothest when the head on the nozzle was one foot or less; therefore, the head on the outer nozzle was kept within this limit. Under this condition the surface of the jet was glassy in appearance. The surface of the inside jet alone was smooth for all velocities, which ranged from 10 to 25 feet per second.

In the course of the water-surface measurements, eight points were read around the jet in 45-degree steps. In this manner, four diameters were determined for each station. It was impossible to determine the exact diameter of the jet at the very edge of the nozzle. Due to surface tension, water jumped the gap of 1/32 inch between the point of the gage and the water jet or the nozzle. For this reason the first station at which diameters were determined was 0.003 foot below the nozzle tip.

Water surfaces were measured as far down the jet as possible. Near the point of complete mixture in the 1 to 1 ratio of discharges of the two nozzles, the water surface was rough and maintained continous contact with the point gage. With the discharge ratios 3/4 to 1 and 1/2 to 1, water-surface measurements were not taken beyond 0.6 foot from the nozzle tip because of the uneven and oscillating character of the surface. Obviously the jets had not attained a thorough mixture at this distance.

Even upon careful visual inspection, it appeared that the outer nozzle flowed full at the tip. However, the data when plotted indicated that because of the sudden change in boundary 0.1 inch

back from the tip of the nozzle, the jet did not expand to follow the nozzle tip.

Velocity traverses of the jets were made with a view to determining the rate of expansion of the inner jet, the location and extent of the mixing zone, and the mixing length.

Dye was injected into the inner nozzle stream to determine the rate of expansion of the inner jet or the rate of mixing of the two streams. An attempt was made to photograph the mixing jets upon the injection of the dye. The photographs offer only general information and a check on the data obtained in the velocity traverses.

Methods of calculation of the shear factor. (a) Computations of shear factor were based on difference in momentum changes of the jets. The following terms are used in the computations:

Sections 0 and X are two transverse sections a distance (dx) apart.

V_{20} = velocity of outer jet at section 0

V_{2X} = velocity of outer jet at section X

V_{10} = velocity of inner jet at section 0

V_{1X} = velocity of inner jet at section X

$$V_1 = \frac{V_{10} + V_{1X}}{2}$$

$$V_2 = \frac{V_{20} + V_{2X}}{2}$$

$dv_1 = V_{10} - V_{1X}$

$dv_2 = V_{20} - V_{2X}$

d_1 = average diameter of inner jet taken from plots

A_1 = average cross-sectional area of inner jet

A = average cross-sectional area of combined jets

F = shear or friction force acting between jets over length (dx)

Treating length (dx) with the impulse or momentum principle, the momentum and forces acting on the inner jet are:

$$\frac{wQ_1 dv_1}{g} + A_1(dp) + wA_1 dx - F = 0 \quad \text{..... (1a)}$$

and on the outer jet

$$\frac{wQ_2 dv_2}{g} + (A - A_1)dp + w(A-A_1)dx + F - dW = 0 \quad \text{..... (1b)}$$

Dividing equation (1a) by A_1 and equation (1b) by $(A - A_1)$ and substracting the second equation from the first, the difference becomes

$$\frac{wQ_1 dv_1}{gA_1} + dp + w(dx) - \frac{F}{A_1} - \frac{wQ_2 dv_2}{g(A - A_1)} - dp - w(dx)$$

$$- \frac{F}{(A - A_1)} - dW = 0.$$

or

$$\frac{wV_1 dv_1}{g} - \frac{wV_2 dv_2}{g} - F\left(\frac{1}{A_1} + \frac{1}{(A - A_1)}\right) - dW = 0.$$

F is a function of the velocity, the area of contact between the two jets, and the viscosity, and can be defined as

$$F = \frac{wX\,(V_1 - V_2)^2 \pi d_1\, dx}{2g}$$

where X = friction factor.

dW, the frictional resistance between the outer jet and the atmosphere is negligibly small and can be assumed to be zero.

Then,

$$\frac{wV_1 dv_1}{g} - \frac{wV_2 dv_2}{g} - \frac{wX(V_1 - V_2)^2 \pi d_1 dx}{2g}\left[\frac{1}{A_1} + \frac{1}{A - A_1}\right] = 0$$

or

$$V_1 dv_1 - V_2 dv_2 - \frac{X}{2}(V_1 - V_2)^2 \pi d_1 dx\left[\frac{1}{A_1} + \frac{1}{(A - A_1)}\right] = 0$$

Therefore,

$$X = \frac{2(V_1 dv_1 - v_2 dv_2)}{(V_1 - V_2)^2 \pi d_1 dx\left[\frac{1}{A_1} + \frac{1}{(A - A_1)}\right]} \quad \text{..... (2)}$$

The velocity traverses shown on figures 3 to 7 indicate fairly well the general boundary between the inner and outer jets, particularly for tests 4 and 7, whose Q ratios were 1 to 1. The photographs of tests 4 and 7, plate II, indicate that the water surface was broken at about station 0+0.3. This demonstrated that the wave of high transverse velocity of the inner jet had reached the surface. At this point all of the discharge of the outer jet apparently had been transferred to the inner jet.

When the discharge of the inner nozzle was reduced in relation to the outer nozzle, its velocity was reduced and therefore transverse wave velocity was likewise reduced. Because of the decreased transverse velocity gradient the mixing length was increased. This is shown in figures 3 to 7 along with plates II to IV.

In the computations for the determination of the friction coefficient, it was necessary to determine the mixing length of the jets. This was done by examination of the velocity distribution curves and the accompanying photographs.

The mixing lengths of tests 4 and 7 were readily determined as 0.3 feet by the above-described method. The mixing lengths of tests 5 and 8 were not so apparent. Upon examination of plate III and the velocity curves in figures 4 and 7, it is hardly possible to say definitely that the two jets were thoroughly mixed within 1-foot distance from the nozzles. However, it appears that the transverse velocity had almost attained a minimum at 1- foot distance. The data are not sufficiently far reaching to show the exact point at which thorough mixing was accomplished. Likewise, in test 6, the mixing length was not clearly defined, figure 5. Plate IV shows that there is a quick change in the appearance of the jet by the small change in discharge ratios from 2/3 to 1 to 3/4 to 1.

Contrasting these velocity curves (figures 4 and 7) with those of test 4 and 7 (figures 3 and 6), it is suggested that perhaps thorough mixing was not attained even in tests 4 and 7, as it does not appear that the transverse velocity gradient is at a minimum even at 0.4-foot distance. In this case, the boundary of the

V-shaped mixing zone intersects the surface of the outer jet before the velocity gradient becomes normal.

In the computations of X by the method previously described, invariably the acceleration of the outer jet as computed was greated than was actually observed in the stream. It may be that either the point at which thorough mixture was attained was in error, or that the trace of the boundary between the jets was not a straight line, but curved. If the mixing lengths were assumed too short, values of X are too large. Due to the very rapid acceleration of the outer jet, the values of X are out of proportion after computations are carried four to six diameters of the small jet. Therefore, the values of X, as computed for the first two or three differential spans, are of greater accuracy.

The following table contains the results of the computations for the shear factor X by means of equation (2). The data used in the computation are tabulated on the next page.

VALUES OF FRICTION FACTOR X

Span feet	Test 4 Q_1 = 0.0395 c.f.s. Q_2 = 0.0395 c.f.s.	Test 6 Q_1 = 0.0296 c.f.s. Q_2 = 0.0395 c.f.s.	Test 7 Q_1 = 0.0365 c.f.s. Q_2 = 0.0362 c.f.s.
0.00 - 0.05	0.159	0.120	0.151
0.05 - 0.10	0.162	0.139	0.157
0.10 - 0.20	0.157	0.131	0.179

Station	Velocity in feet per second $\mathcal{C}_L$	0.1"	0.20"	0.25"	0.30"	0.35"	0.40"	0.45"	Diameter of jet in inches 0°	45°	90°	135°	Mean	Span	X
					Test 4, Q_1 = 0.0395 c.f.s.; Q_2 = 0.0395 c.f.s.										
0.000	24.13	24.11	24.03	23.63	7.39	7.82	7.82	7.78	-	-	-	-	-	0.000	-
.003	-	-	-	-	-	-	-	-	1.130	1.133	1.123	1.127	1.128	-	0.159
.025	-	-	-	-	-	-	-	-	1.092	1.101	1.092	1.096	1.095	-	
.050	24.19	24.10	24.03	22.36	13.77	8.06	7.94	7.98	1.079	1.080	1.076	1.080	1.079	0.050	0.162
.100	24.13	24.17	24.12	21.42	15.59	8.75	8.30	8.18	1.059	1.064	1.058	1.063	1.061	0.100	
.150	-	-	-	-	-	-	-	-	1.045	1.046	1.040	1.053	1.046	-	0.157
.200	24.21	24.23	23.54	20.18	15.55	12.03	9.69	8.49	1.052	1.024	1.028	1.045	1.037	0.200	
.300	24.38	24.44	23.21	19.28	16.36	13.89	12.00	9.45	1.031	1.069	1.046	1.045	1.048	-	
.400	24.38	24.00	23.34	18.80	16.79	14.61	13.32	10.91	-	-	-	-	-	-	
					Test 6, Q_1 = 0.0296 c.f.s.; Q_2 = 0.0395 c.f.s.										
0.000	17.20	17.08	16.80	16.86	7.84	7.82	7.82	7.84	-	-	-	-	-	0.000	-
.003	-	-	-	-	-	-	-	-	1.136	1.143	1.143	1.138	1.140	-	0.120
.025	-	-	-	-	-	-	-	-	1.116	1.114	1.108	1.111	1.112	-	
.050	17.26	17.16	16.90	15.90	8.35	8.04	8.02	8.04	1.107	1.108	1.100	1.106	1.105	0.050	0.139
.100	17.31	17.26	16.99	14.92	9.97	8.26	8.22	8.24	1.082	1.075	1.089	1.086	1.083	0.100	
.150	-	-	-	-	-	-	-	-	1.074	1.072	1.089	1.079	1.078		0.131
.200	17.45	17.46	17.18	14.53	11.58	9.32	8.60	8.62	1.077	1.063	1.078	1.072	1.072	0.200	
.250	-	-	-	-	-	-	-	-	1.067	1.036	1.078	1.055	1.059		
.300	17.63	17.64	17.37	14.49	12.45	10.45	9.28	9.02	1.060	1.046	1.073	1.040	1.054		
.400	17.81	17.84	17.39	14.56	12.78	11.32	10.18	9.45	1.037	1.022	1.063	1.043	1.041		
.500	17.98	17.83	17.59	14.57	13.06	12.10	10.79	10.21	-	-	-	-	-		
.600	17.96	17.48	16.94	14.61	13.41	12.24	11.51	10.52	-	-	-	-	-		
					Test 7, Q_1 = 0.0365 c.f.s.; Q_2 = 0.0362 c.f.s.										
0.000	21.69	21.87	21.86	21.62	6.80	7.06	7.06	7.02	-	-	-	-	-	0.000	-
.003	-	-	-	-	-	-	-	-	1.132	1.127	1.125	1.125	1.127	-	0.151
.025	-	-	-	-	-	-	-	-	1.088	1.089	1.087	1.093	1.089	-	
.050	21.74	21.73	21.86	20.85	10.37	7.31	7.28	7.24	1.070	1.093	1.071	1.074	1.077	0.050	0.157
.100	21.89	21.89	21.90	19.23	16.94	7.57	7.50	7.46	1.046	1.047	1.043	1.048	1.046	0.100	
.150	-	-	-	-	-	-	-	-	1.043	1.028	1.024	1.039	1.033	-	0.179
.200	22.00	22.00	21.14	18.13	14.28	10.46	8.18	7.88	1.025	1.000	1.019	1.021	1.016	0.200	
.250	-	-	-	-	-	-	-	-	1.013	0.994	1.020	1.019	1.012		
.300	22.14	22.13	20.11	17.57	14.74	12.16	10.02	8.54	0.997	1.024	1.022	1.024	1.017		
.400	22.28	22.05	19.28	17.35	15.45	13.20	11.43	9.69	-	-	-	-	-		
.500	21.98	21.39	18.77	17.18	15.86	13.70	12.40	10.82	-	-	-	-	-		
.600	20.67	20.21	18.02	16.82	15.70	14.20	-	-	-	-	-	-	-		

IV. DETERMINATION OF EFFECT OF SHAPE OF DRIVING NOZZLE ON MOMENTUM TRANSFER OR PUMP EFFICIENCY

It is established that the momentum of the driving jet of a jet pump is transferred to the driven jet through the mechanics of friction or shear between the two jets. The friction or shearing force between these two jets acts on an area of contact of the jets. It was thought that if the area of contact between the jets is increased, the rate of transfer of energy would be increased, or a thorough mixing could be accomplished in a shorter mixing tube, or better yet, a greater percentage of momentum transfer could be effected. This latter possibility was the basis of the investigation.

To determine the effect of the circumference and shape of the driving jet upon the efficiency of a pump, a number of driving nozzles were designed and built all with approximately the same cross-sectional area but with widely different shape and circumferences. All of these nozzles were operated with the same entraining nozzle and in connection with a mixing chamber, in order that the nozzles would function as a pump.

Figure 8 and plate V shows the general arrangement of the laboratory apparatus. The details of the nozzle assembly were essentially the same as used in the jet tests described in part I and are shown on figure 9. The water supply was taken from the city water supply at 80 pounds per square inch. In each of the supply lines was placed an orifice which was calibrated gravimetrically for discharge at various pressure drops across the orifice. Discharge curves were drawn for each supply line. The static head on the outer nozzle was maintained at a constant value throughout the entire series of tests. This head was the minimum head at which no disturbance due to eddies and vortices occurred.

The various types of nozzles tried are shown on figures 10 to 13 in their positions relative to the outer nozzles. The mixing tube is not shown. Plate VI shows most of these nozzles. The nozzles whose numbers do not appear in figures 10 to 13 were not tested because they were throught to be infeasible for various reasons.

Data observed on the various types of driving nozzles are shown in plotted form on figures 14 to 20. For the purpose of comparison, the input and output of the various combinations of nozzles are shown in plotted form on figure 14.

The input and output in foot-pounds per second were computed for each nozzle. The input was considered to be the energy in the water at the base of the inner nozzle and was equal to:

$$Q_1 w \left[\frac{V_1^2}{2g} + h_1 \right]$$

where

Q_1 = discharge of inner nozzle

$\frac{V_1^2}{2g}$ = velocity head in pipe

h_1 = static head at base of nozzle

The output was considered to be the energy in the water actually pumped; that is, the amount of water that would come through the outer nozzle when the inner nozzle was shut off was deducted from the total discharge of the outer nozzle. It is apparent that the value deducted was not constant when the inner nozzle was discharging but it was considered close enough for comparative purposes. By following this method, any changes in the discharge of the outer nozzle due to slight changes in area in the different nozzles were compensated. The output, therefore, was

$$(Q_2 - Q_g) \cdot \frac{wV^2}{2g}$$

where

Q_2 = discharge of the outer nozzle

Q_g = discharge of outer nozzle when acting alone

$\frac{V^2}{2g}$ = velocity head of water discharging from pyralin tube

A sample computation for type I is shown below.

$Q_g = 0.0686$, $Q_1 = 0.0582$, $Q_2 = 0.0817$, $h_1 = 17.40$

Area at base of inner nozzle = 0.006 sq. ft.

Area of pyralin tube = 0.0069 sq. ft.

$$V_1 = \frac{Q_1}{A_1} = \frac{0.0582}{0.006} = 9.70 \text{ feet per second}$$

$$\text{Input} = Q_1 w\left(\frac{V_1^2}{2g} + h\right) = 0.0582 \times 62.4\left(\frac{9.7^2}{64.4} + 17.4\right) = 69.0 \frac{\text{ft.lbs.}}{\text{sec.}}$$

$$V = \frac{Q_1 + Q_2}{0.0069} = \frac{0.0582 + 0.0817}{0.0069} = 20.28 \text{ feet per second}$$

$$\text{Output} = (Q_2 - Q_g)\, w \frac{V^2}{2g} = (0.0817 - 0.0686) \times 62.4 \times \frac{20.28^2}{64.4}$$

$$= 5.22 \frac{\text{ft.lbs.}}{\text{sec.}}$$

It was natural to use type I as a basis of comparison for the other nozzles. The performance of this nozzle is relatively good and its coefficient of discharge is relatively high, 0.99.

Type II nozzle, consisting of a hollow cone from which the water flowed through the small holes, performed very poorly. The jets from these holes were so small that they broke up immediately outside of the nozzle. The jets emerged from the nozzles, not parallel to the axis, but divergent from the axis. Because of this fact, much energy was dissipated before the driving jets contacted the driven jet. The head loss in this nozzle was excessively high, the coefficient of discharge being only 0.77.

Type IV had a favorable coefficient of discharge of 0.94. Unlike type II, it did not distort the shape of the outer jet much when operating without the mixing tube and it appeared to shorten the mixing length somewhat as compared with the circular nozzle. It did not pump as well as the circular nozzle. The circumference of type IV was 1.6 times that of the circular nozzle. Inasmuch as the jet from this nozzle was not as symmetrical as possible, type V was developed and constructed.

The circumference of type V was nearly 2.6 times that of the circular nozzle with the same cross-sectional area. The discharge coefficient was 0.93, nearly that of type IV. When operated alone, this nozzle formed a sharply defined jet after the pattern of the nozzle. When the two nozzles were operated together, without the pyralin mixing tube, the outer jet appeared smooth and much like that of the circular nozzle. The discharge required to pump a unit of water with type V was less than for any other of the nozzles tested.

Type XI. A nozzle was developed in which the driving water flowed between two concentric tubes, the driven water flowing inside as well as outside of this jet. The total circumference of contact between the driving jet and the driven jet was 2.3 times that of type I nozzle. The head loss in this nozzle was quite high due to the sharp bends in the tubing, poor entrance conditions, and the relatively high friction in the tubes. The discharge coefficient was 0.79 and the delivery of pumped water was low.

Type XII was constructed using the same principle as in type XI. The entrance conditions were improved by tapering the tubes and rounding the entrances and by using larger pipe in the entrance chamber. The coefficient of discharge of this nozzle is 0.95. The efficiency as a pump was increased over that of type XI, but it still did not compare favorably with the circular nozzle.

Type VIII and type IX, shown on figure 10, were tried next. The head losses were high in the nozzle and they appeared to pump very little; a complete set of data was not recorded on these nozzles.

- - -

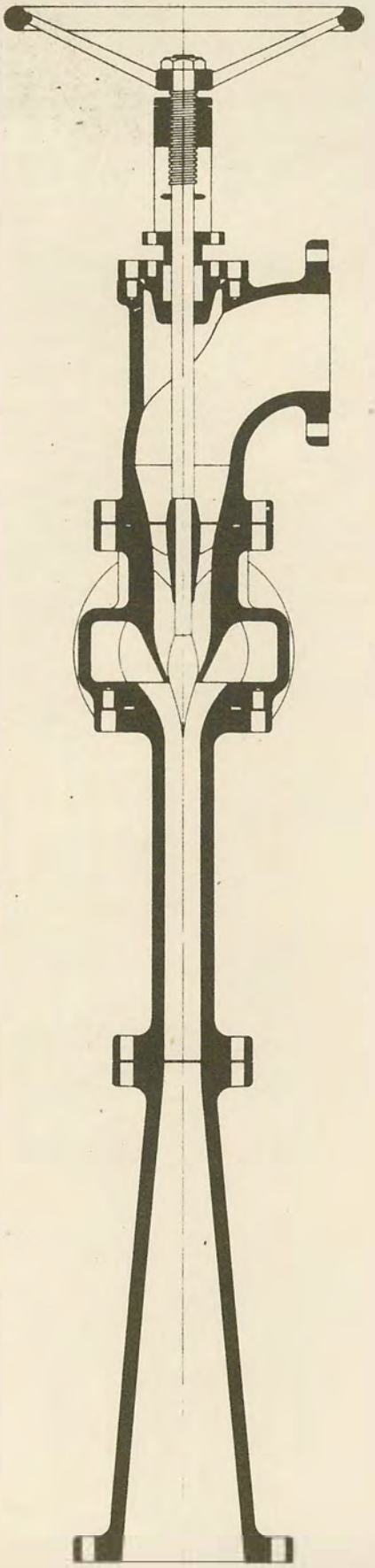

JET PUMP

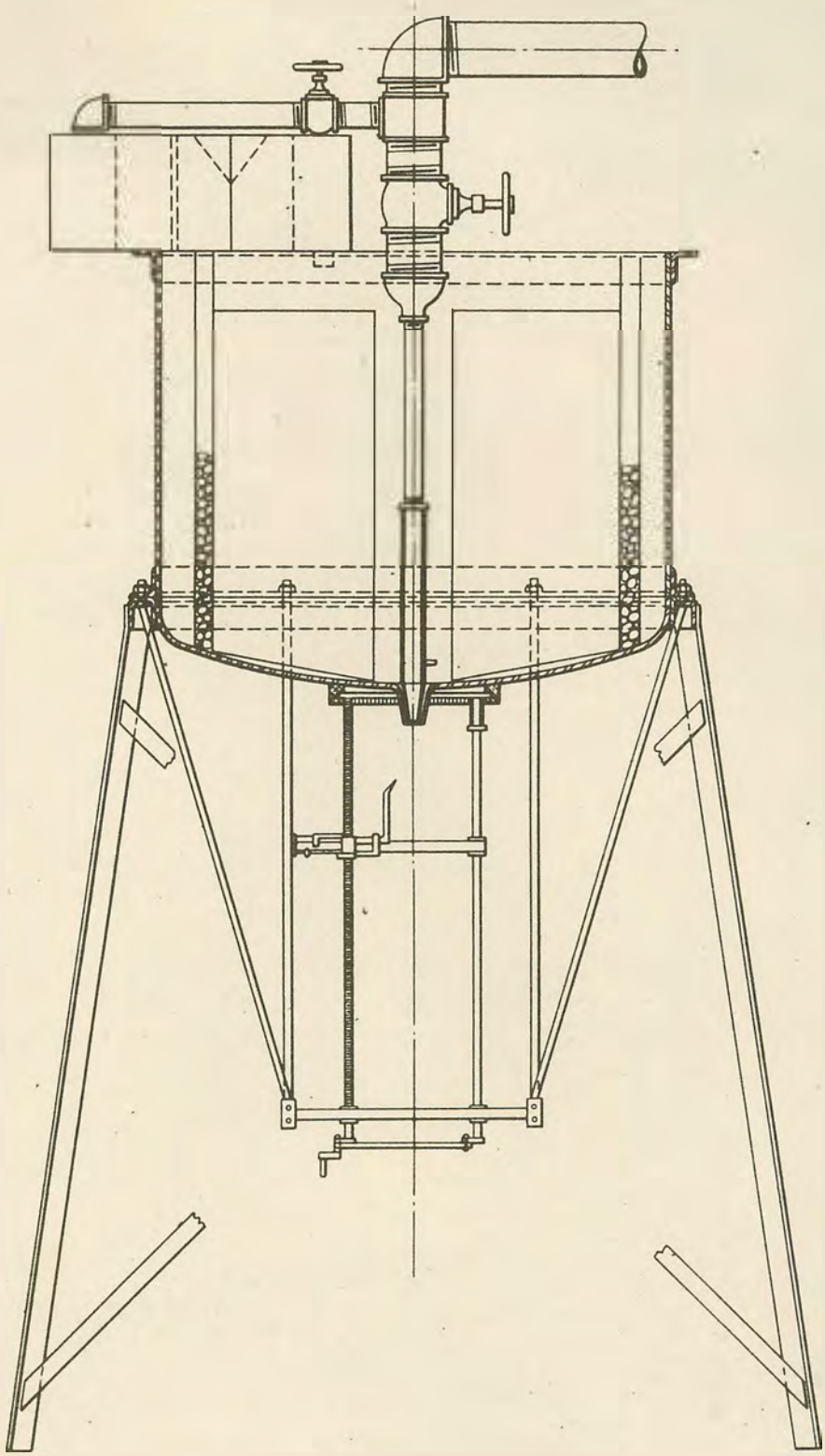

LABORATORY SETUP FOR JET TESTS

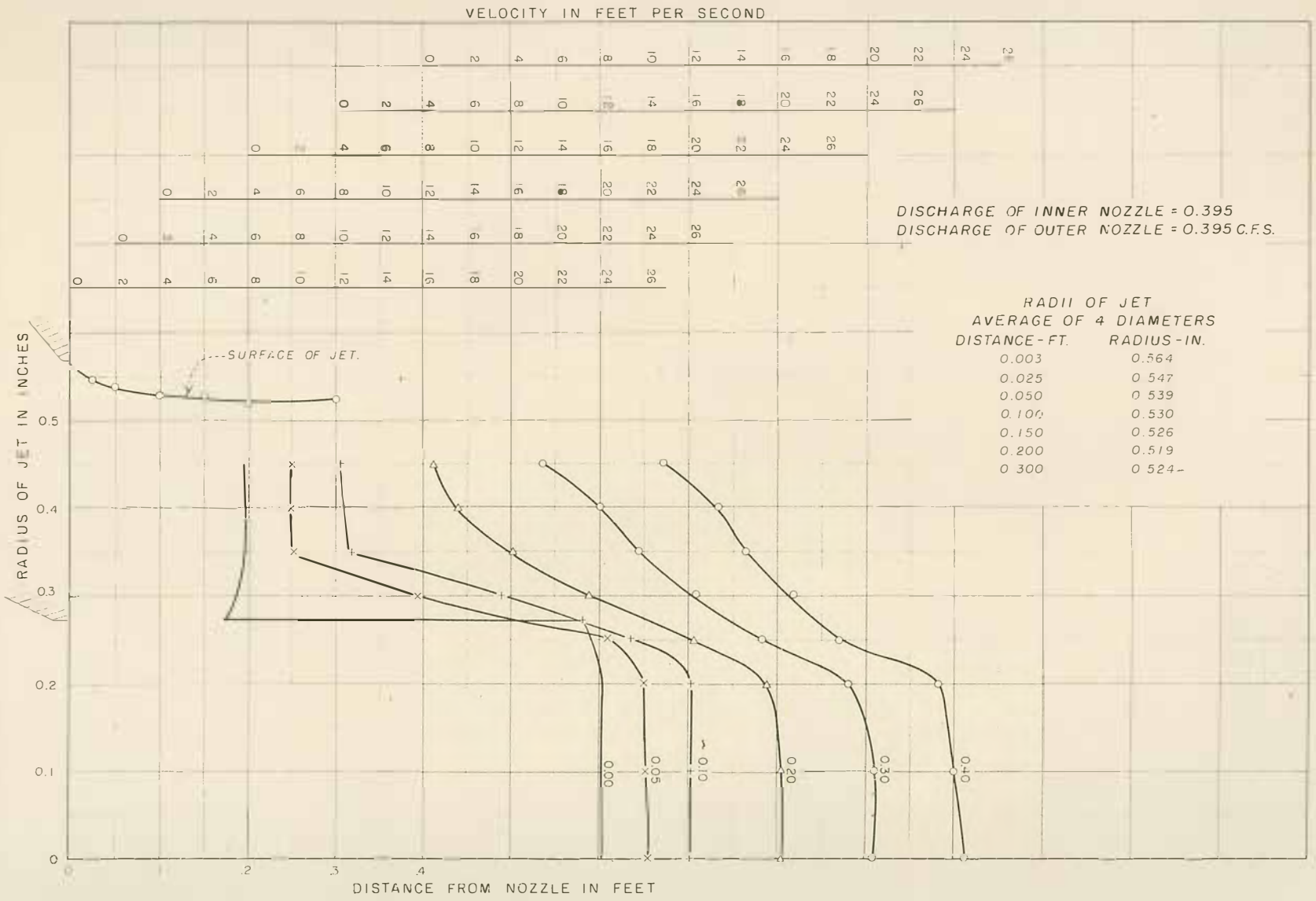

PROFILE OF OUTER JET AND VELOCITY DISTRIBUTION OF MIXING JETS

TEST No. 4

FIGURE 3

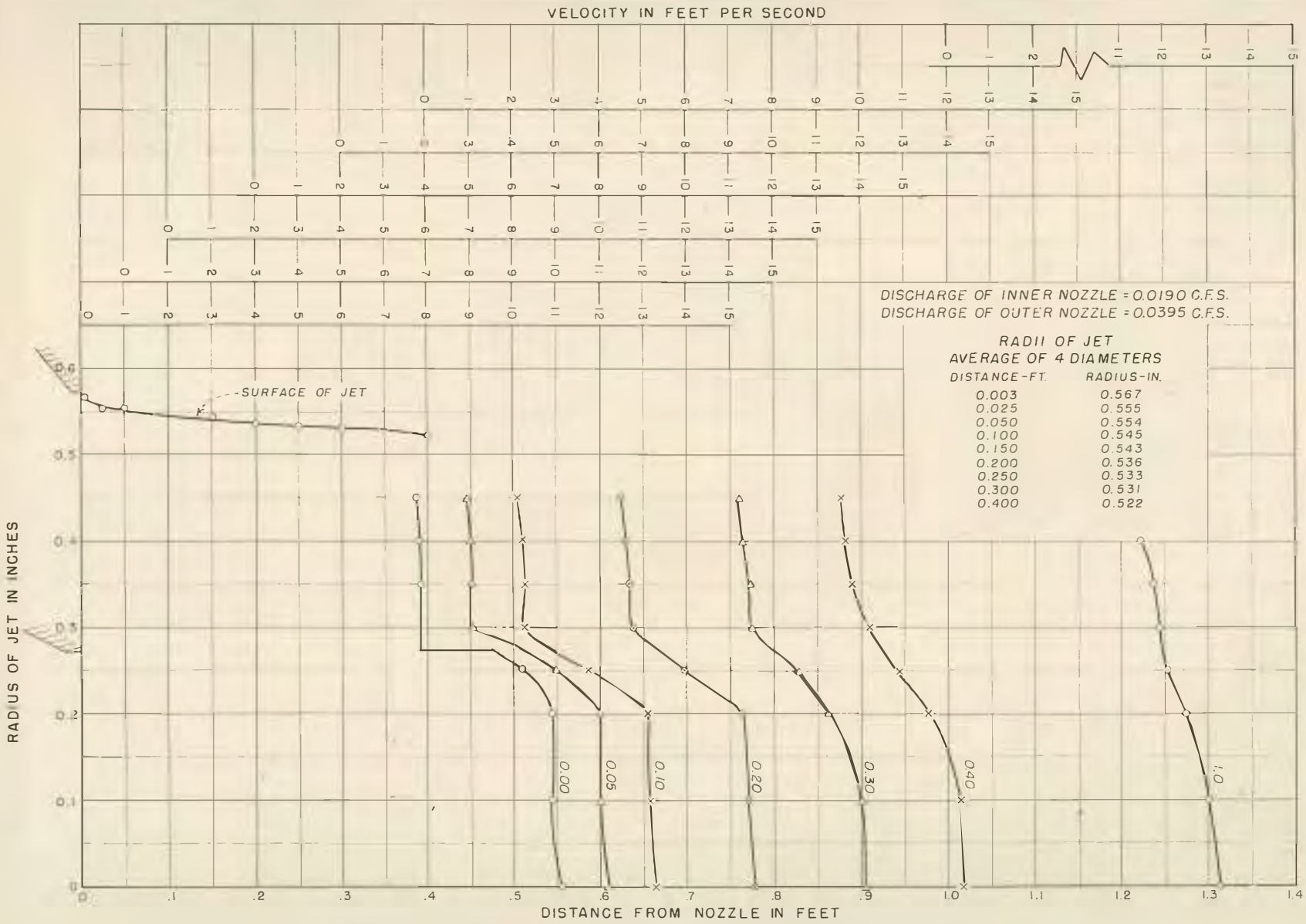

PROFILE OF OUTER JET AND VELOCITY DISTRIBUTION OF MIXING JETS
TEST No. 5

FIGURE 4

HYD-97

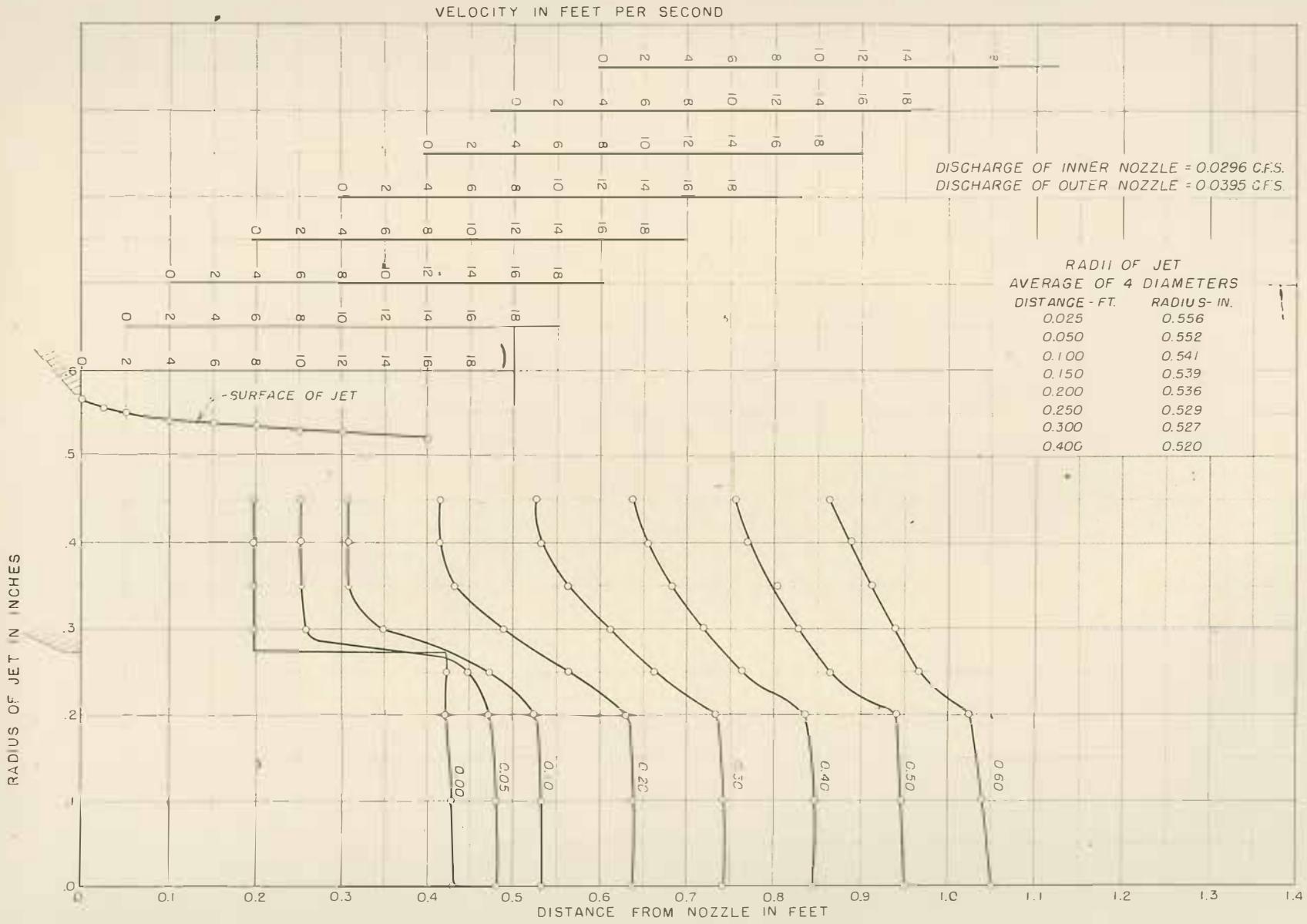

PROFILE OF OUTER JET AND VELOCITY DISTRIBUTION OF MIXING JETS

TEST No. 6

FIGURE 5

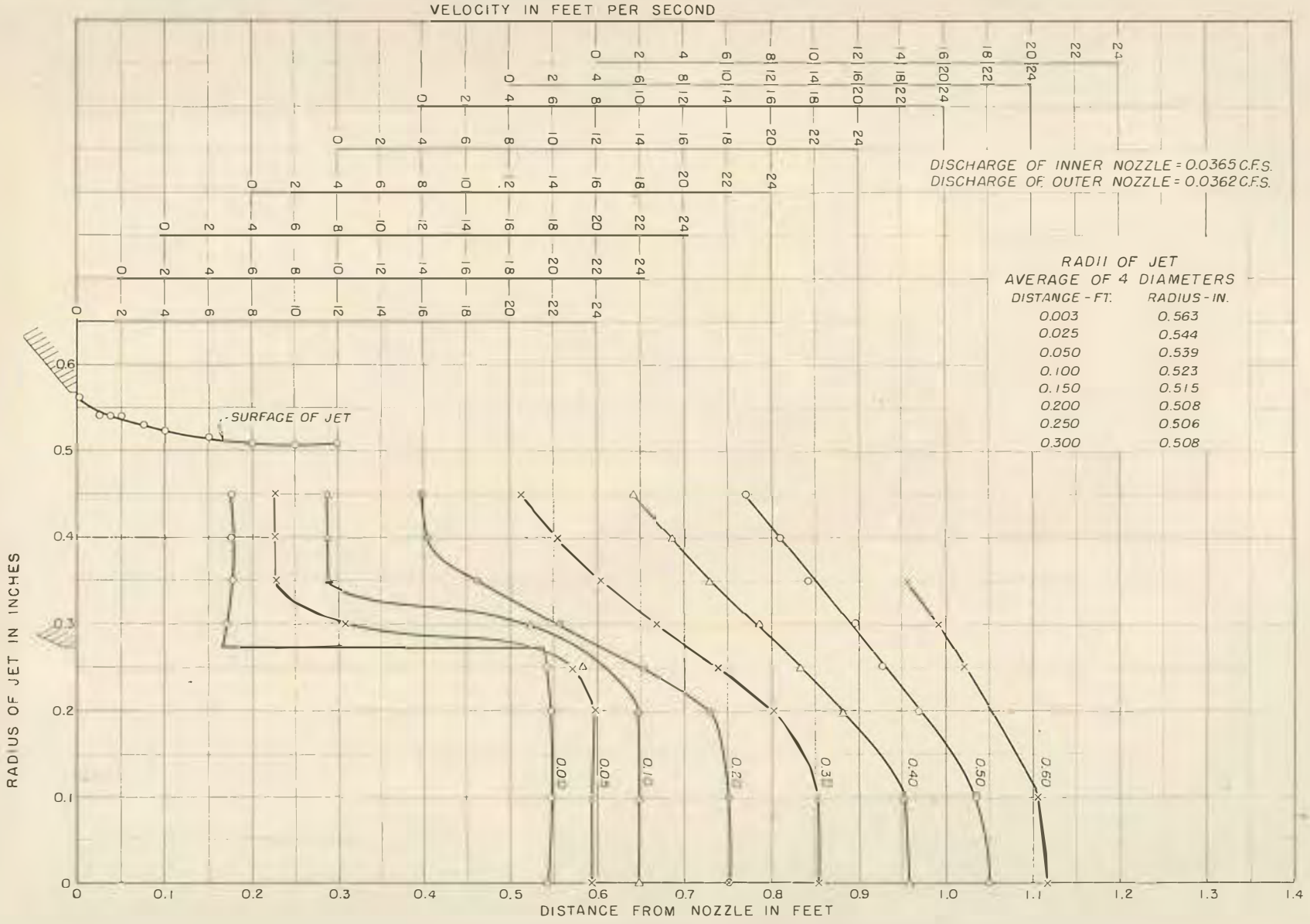

PROFILE OF OUTER JET AND VELOCITY DISTRIBUTION OF MIXING JETS
TEST No. 7

FIGURE 6

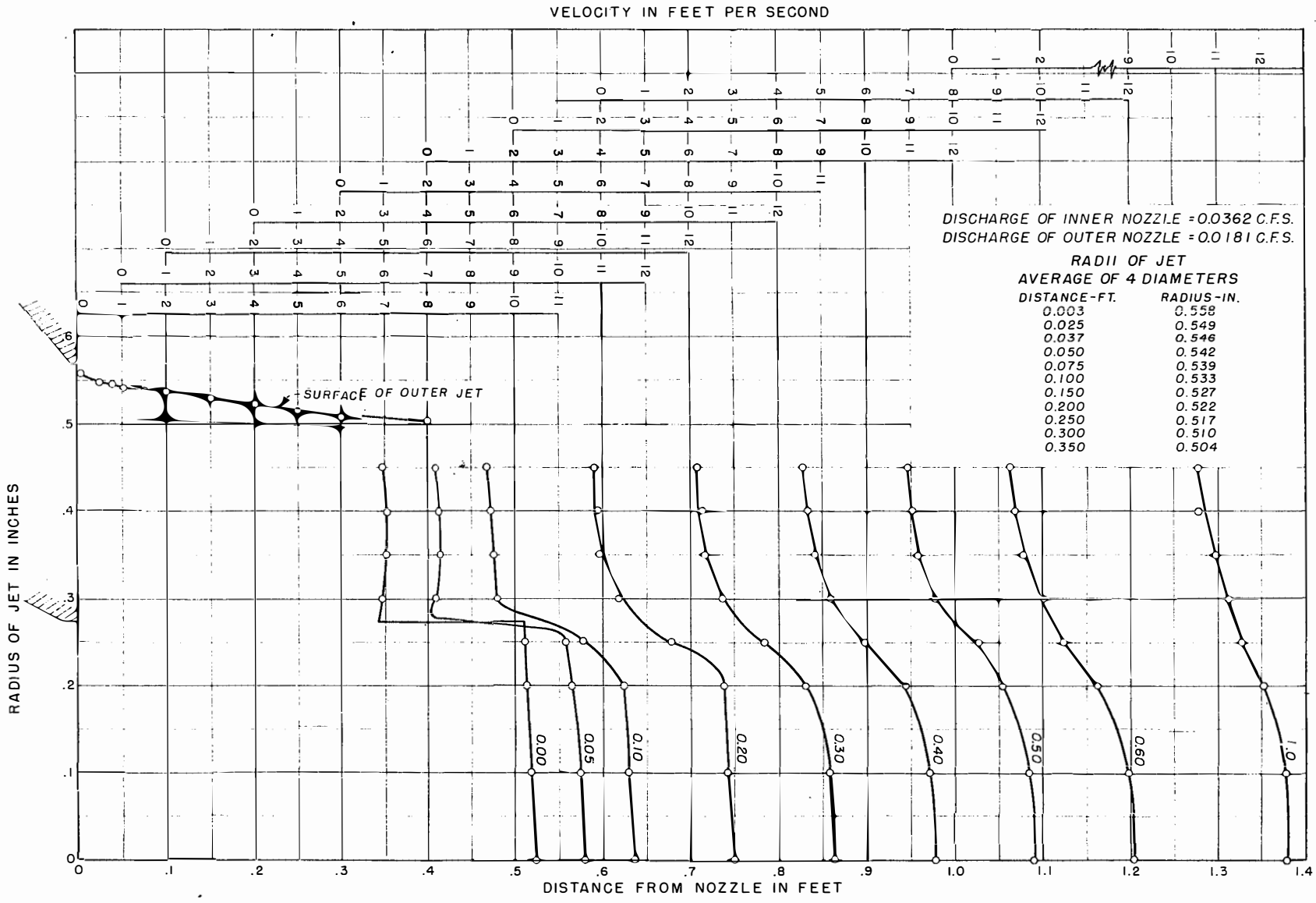

PROFILE OF OUTER JET AND VELOCITY DISTRIBUTION OF MIXING JETS
TEST No. 8

FIGURE 7

HYD-97

LABORATORY SET-UP FOR JET TESTS

FIGURE 6

FIGURE 9

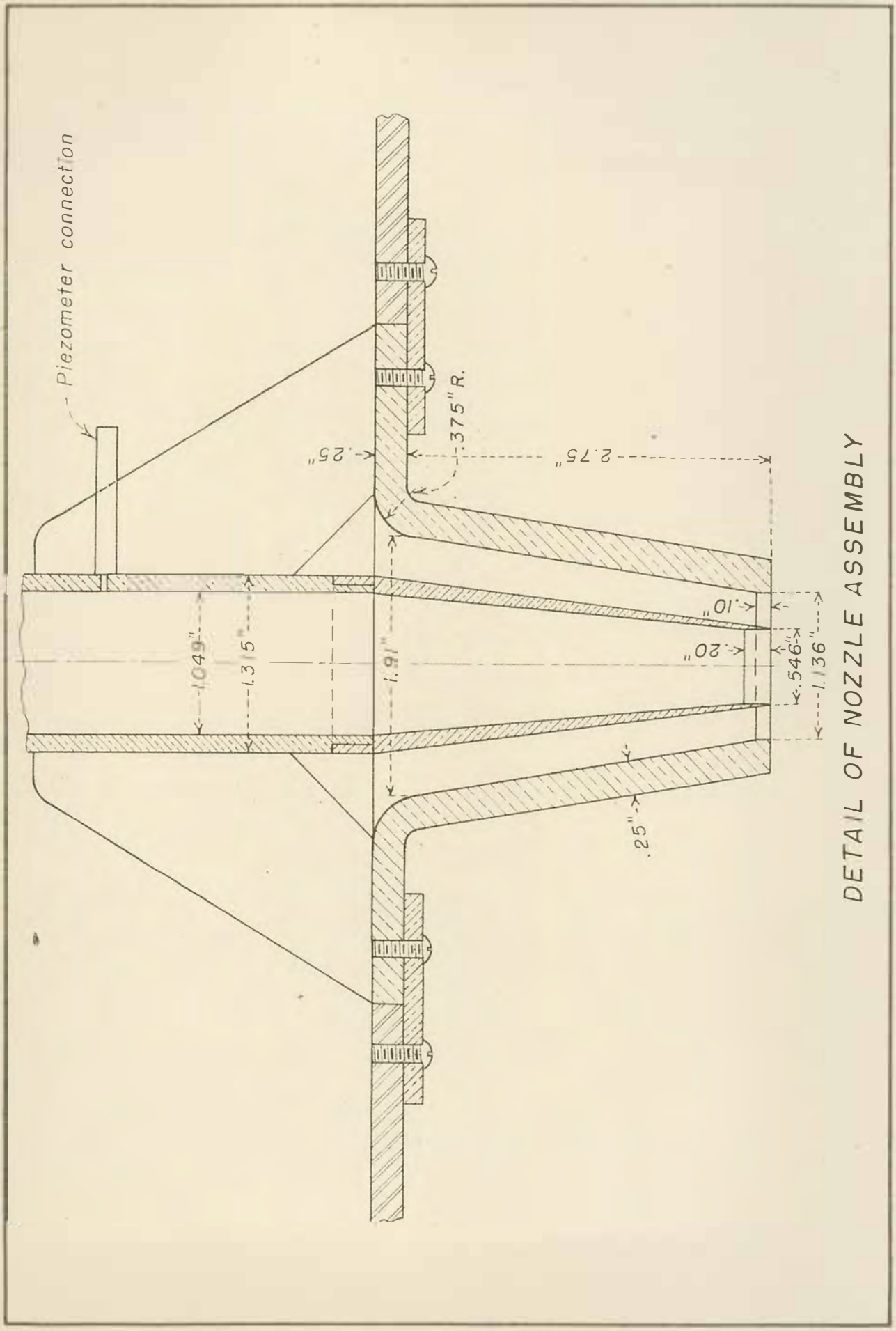

DETAIL OF NOZZLE ASSEMBLY

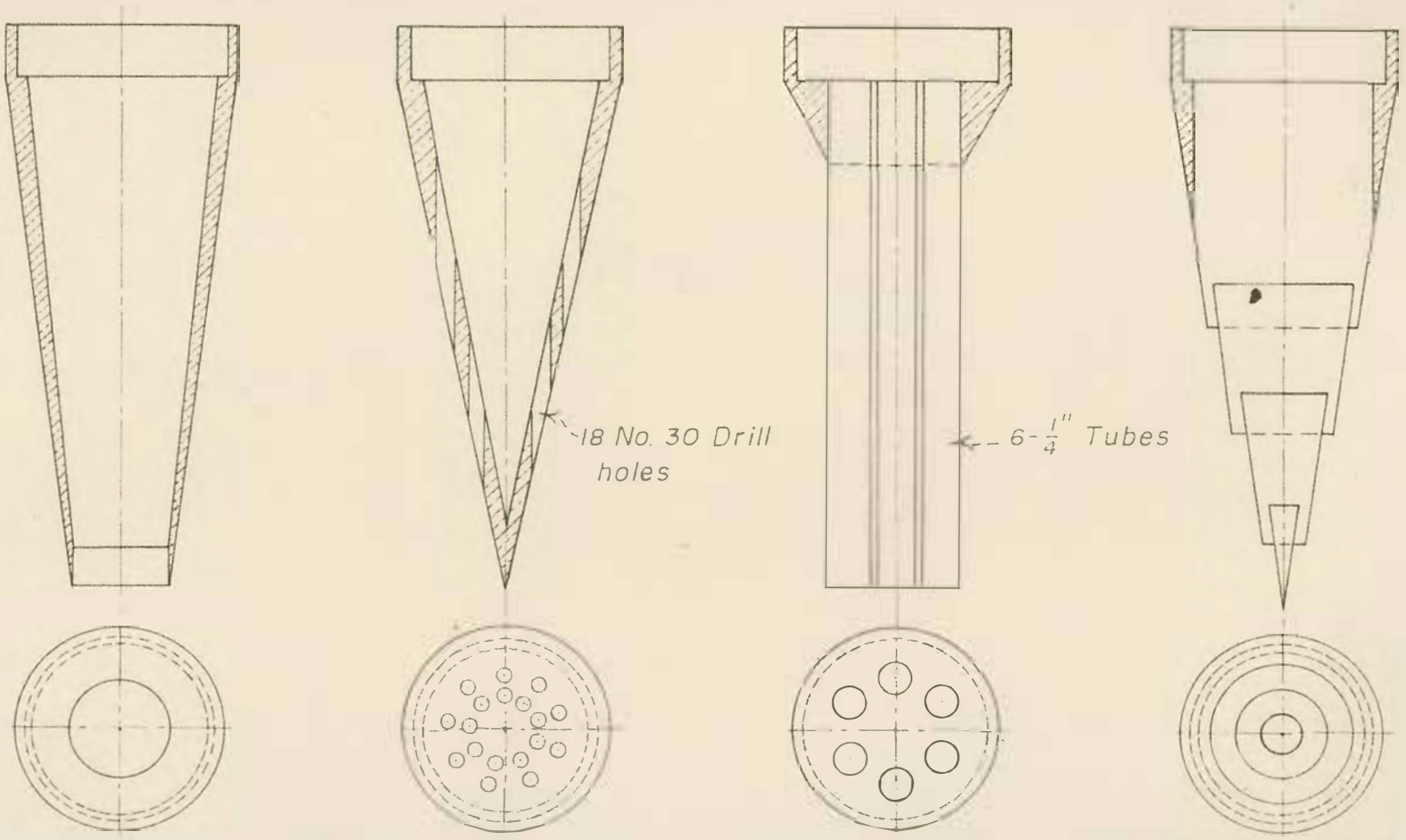

TYPE I
AREA = .234 SQ IN.

TYPE II
AREA = .233 SQ. IN.

TYPE VIII
AREA = .225 SQ. IN.

TYPE IX
AREA = .234 SQ. IN.

TYPES OF NOZZLES USED IN JET TESTS

FIGURE 10

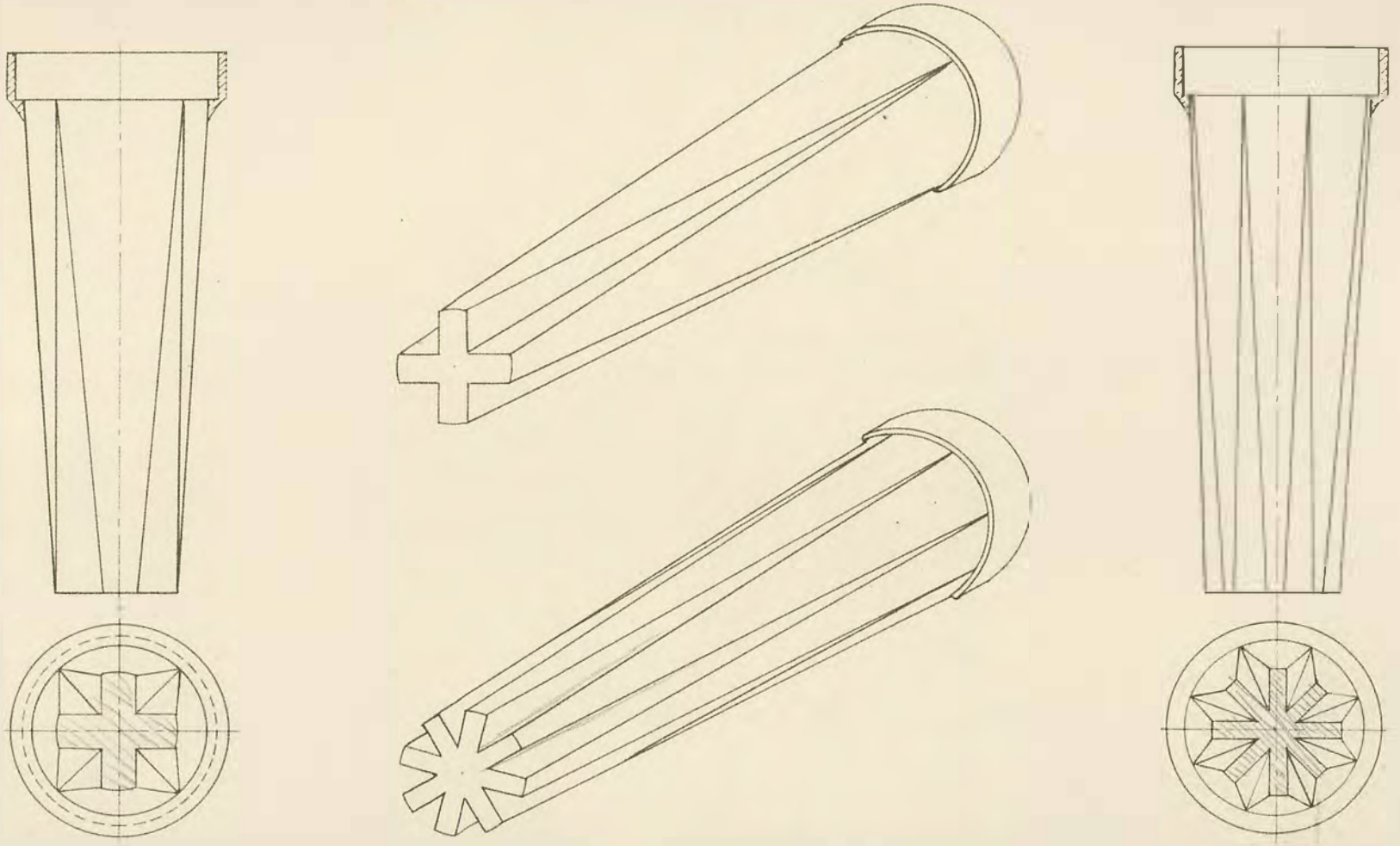

TYPE IV
AREA = 294 SQ. IN.

TYPE V
AREA = .238 SQ. IN.

TYPES OF NOZZLES USED IN JET TESTS

FIGURE 11

FIGURE 12

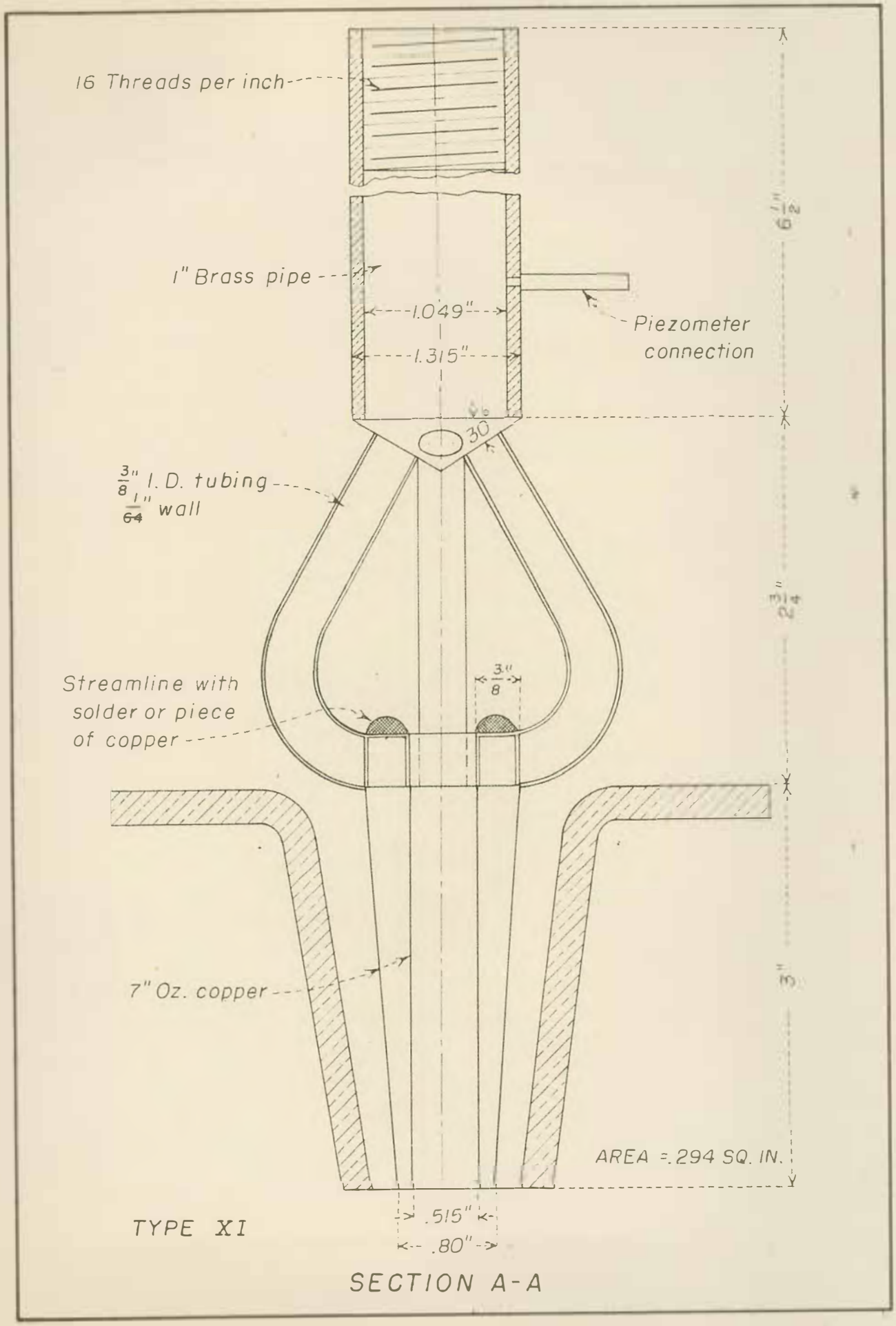

SECTION A-A

FIGURE 13

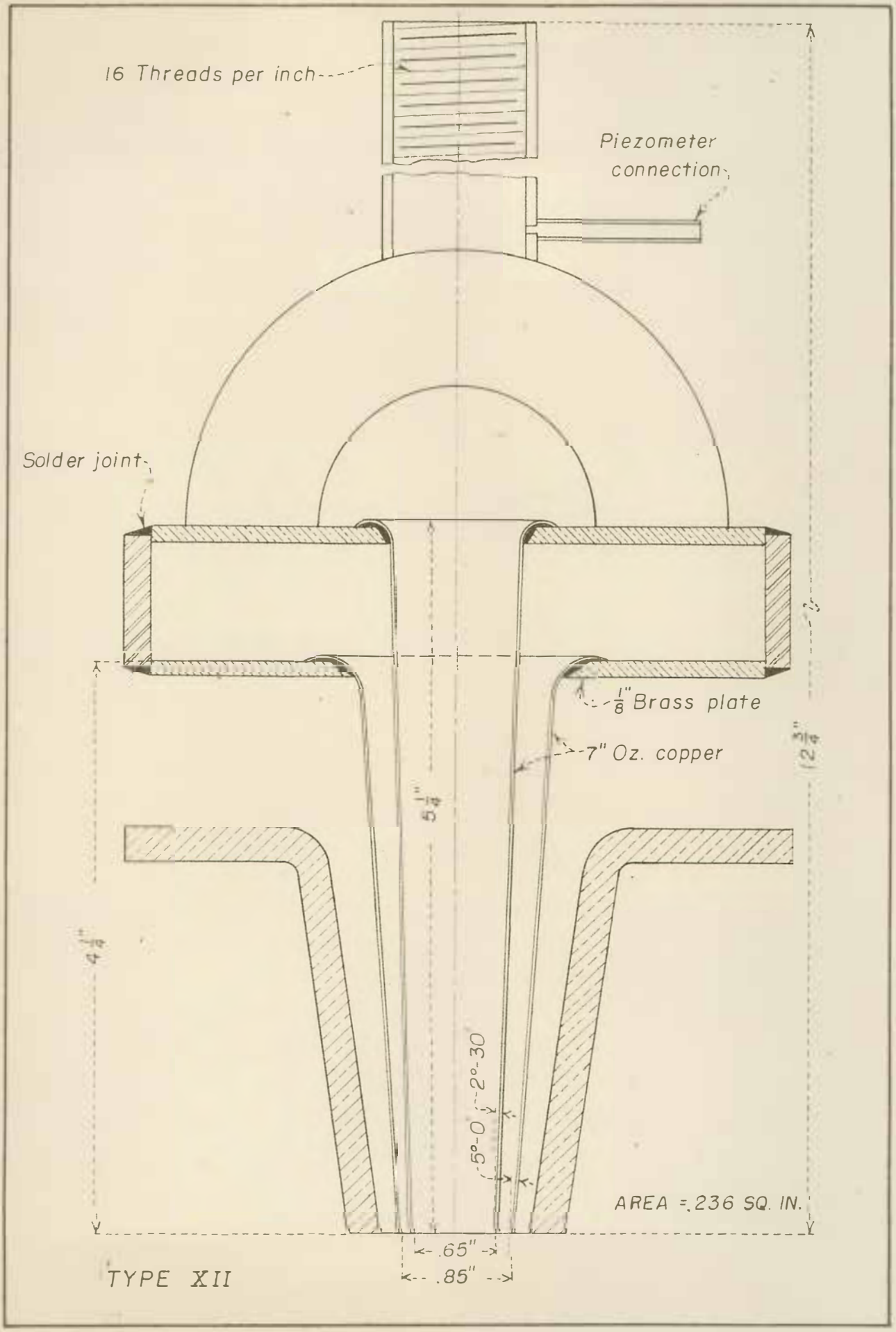
16 Threads per inch
Piezometer connection
Solder joint
1/8" Brass plate
7" Oz. copper
5 1/4"
2 3/4"
4 1/4"
2°-30'
5°-0'
AREA = .236 SQ. IN.
.65"
.85"
TYPE XII

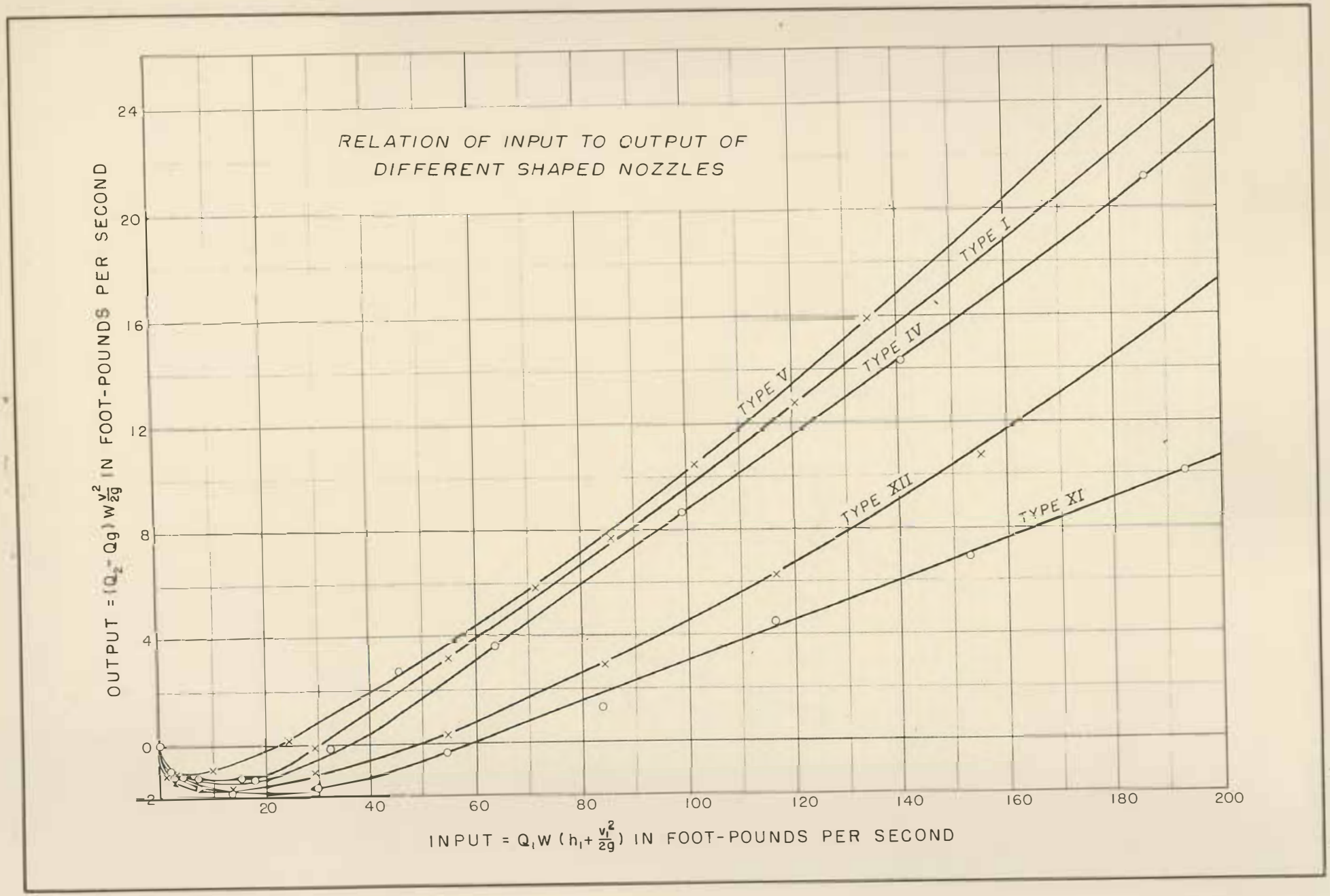
RELATION OF INPUT TO OUTPUT OF
DIFFERENT SHAPED NOZZLES
TYPE I
TYPE IV
TYPE V
TYPE XII
TYPE XI
OUTPUT = $(Q_2 - Q_g) w \frac{v^2}{2g}$ IN FOOT-POUNDS PER SECOND
INPUT = $Q_1 W (h_1 + \frac{v_1^2}{2g})$ IN FOOT-POUNDS PER SECOND
24
20
16
12
8
4
0
-2
20
40
60
80
100
120
140
160
180
200

FIGURE 14

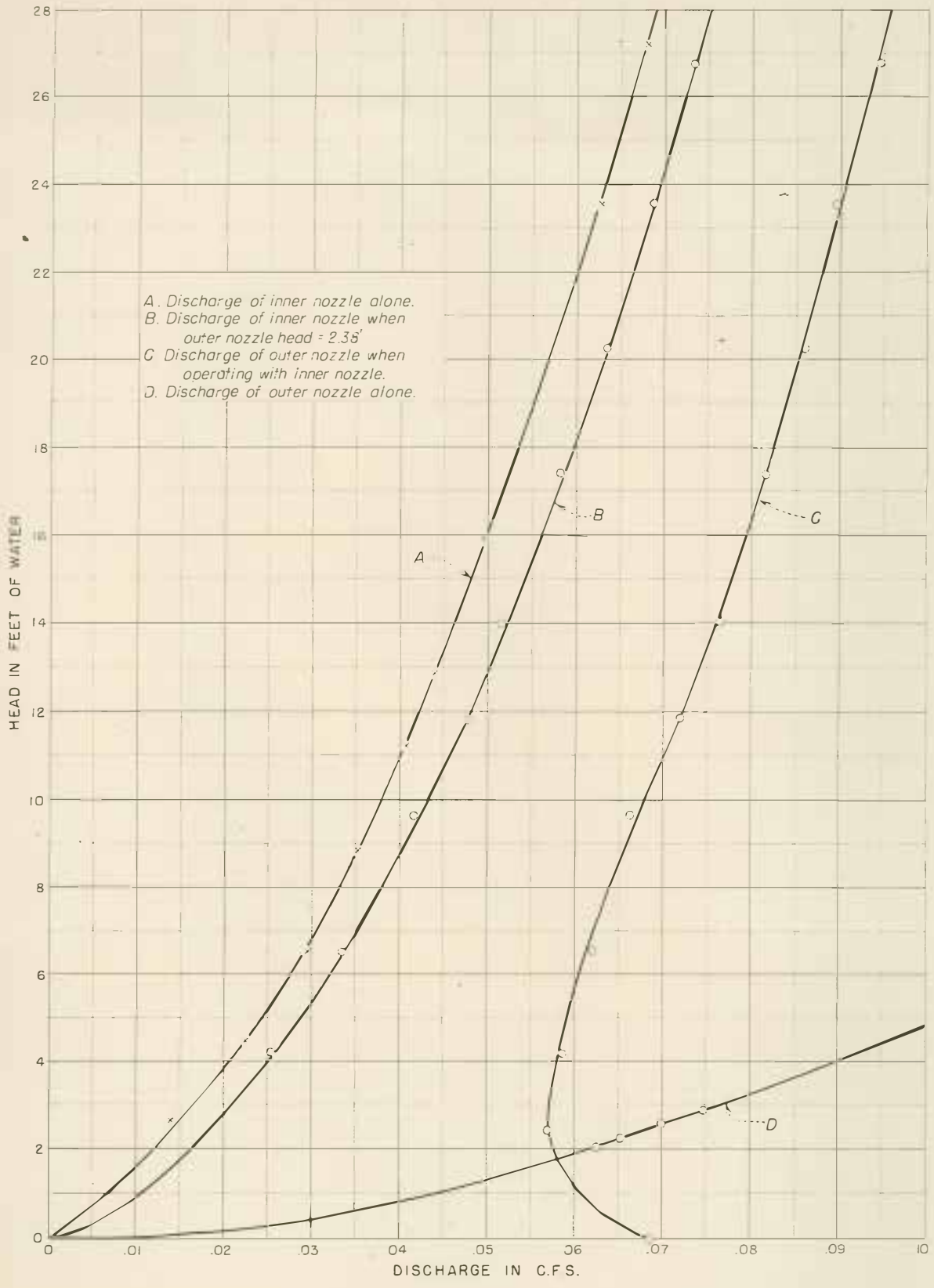

CHARACTERISTICS OF TYPE I INNER NOZZLE

AVERAGE COEFFICIENT OF DISCHARGE = 0.99

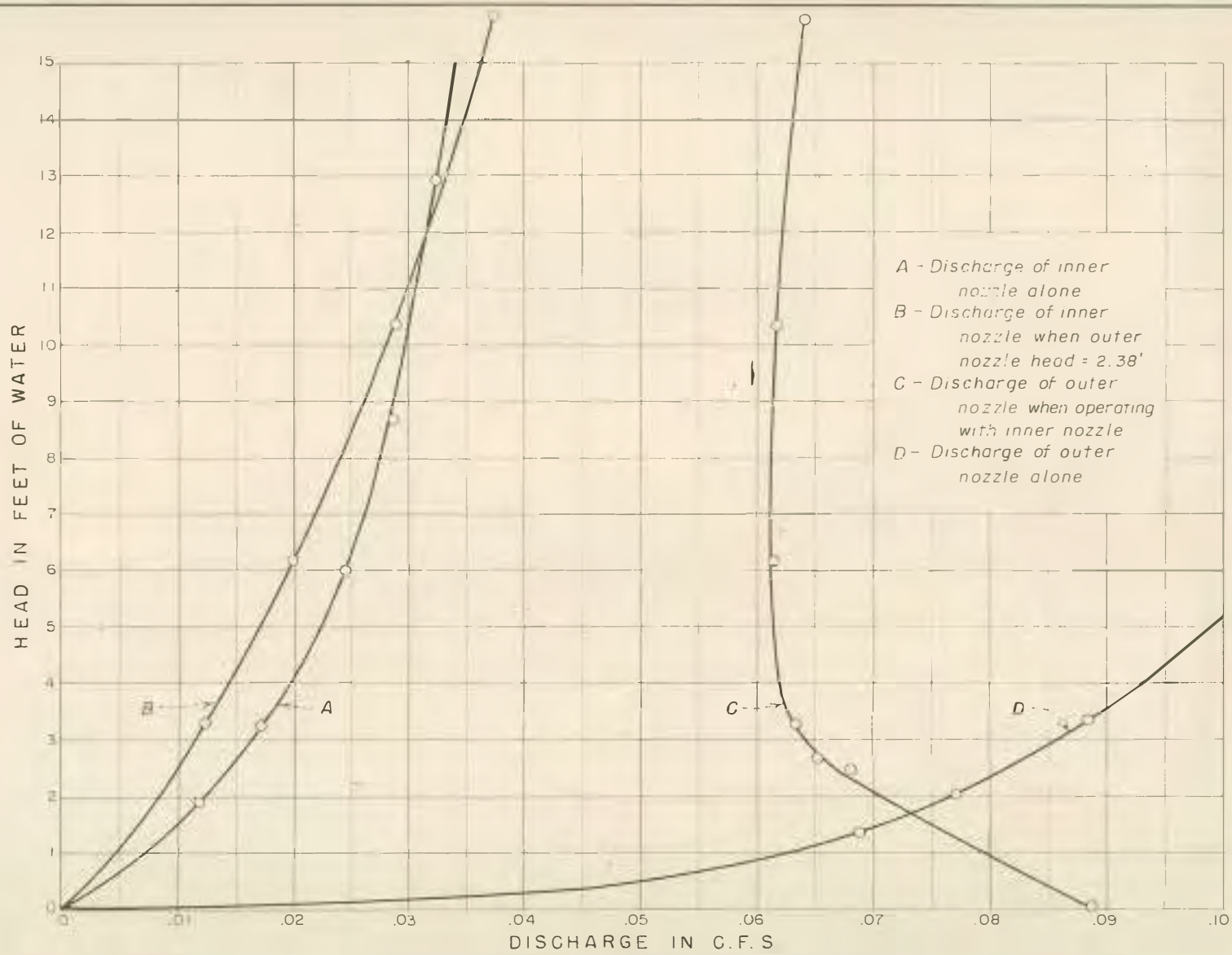

CHARACTERISTICS OF TYPE II INNER NOZZLE

AVERAGE COEFFICIENT OF DISCHARGE = 0.76

FIGURE 16

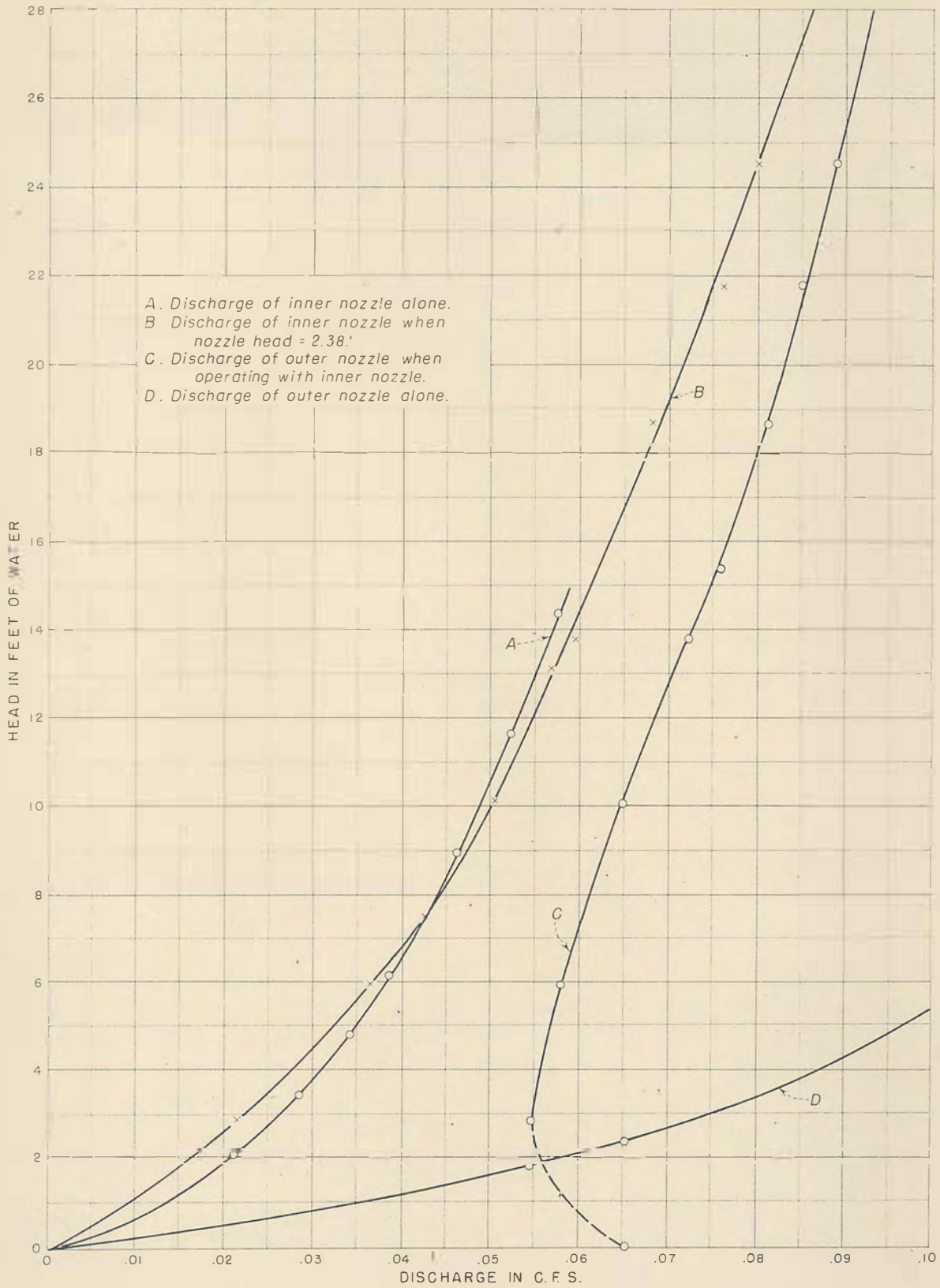

CHARACTERISTICS OF TYPE IV INNER NOZZLE

AVERAGE COEFFICIENT OF DISCHARGE = 0.94

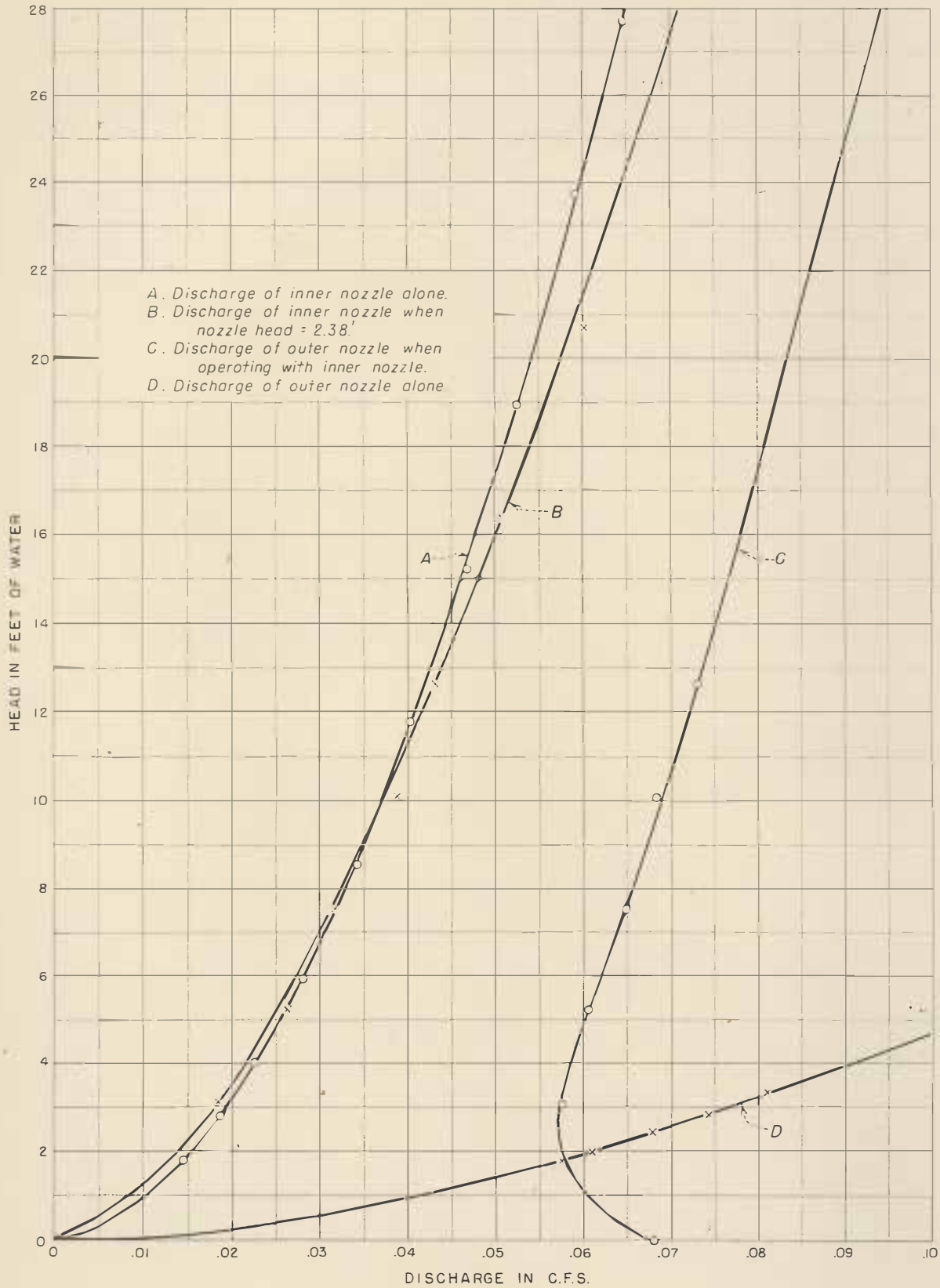

CHARACTERISTICS OF TYPE V INNER NOZZLE

AVERAGE COEFFICIENT OF DISCHARGE = 0.93

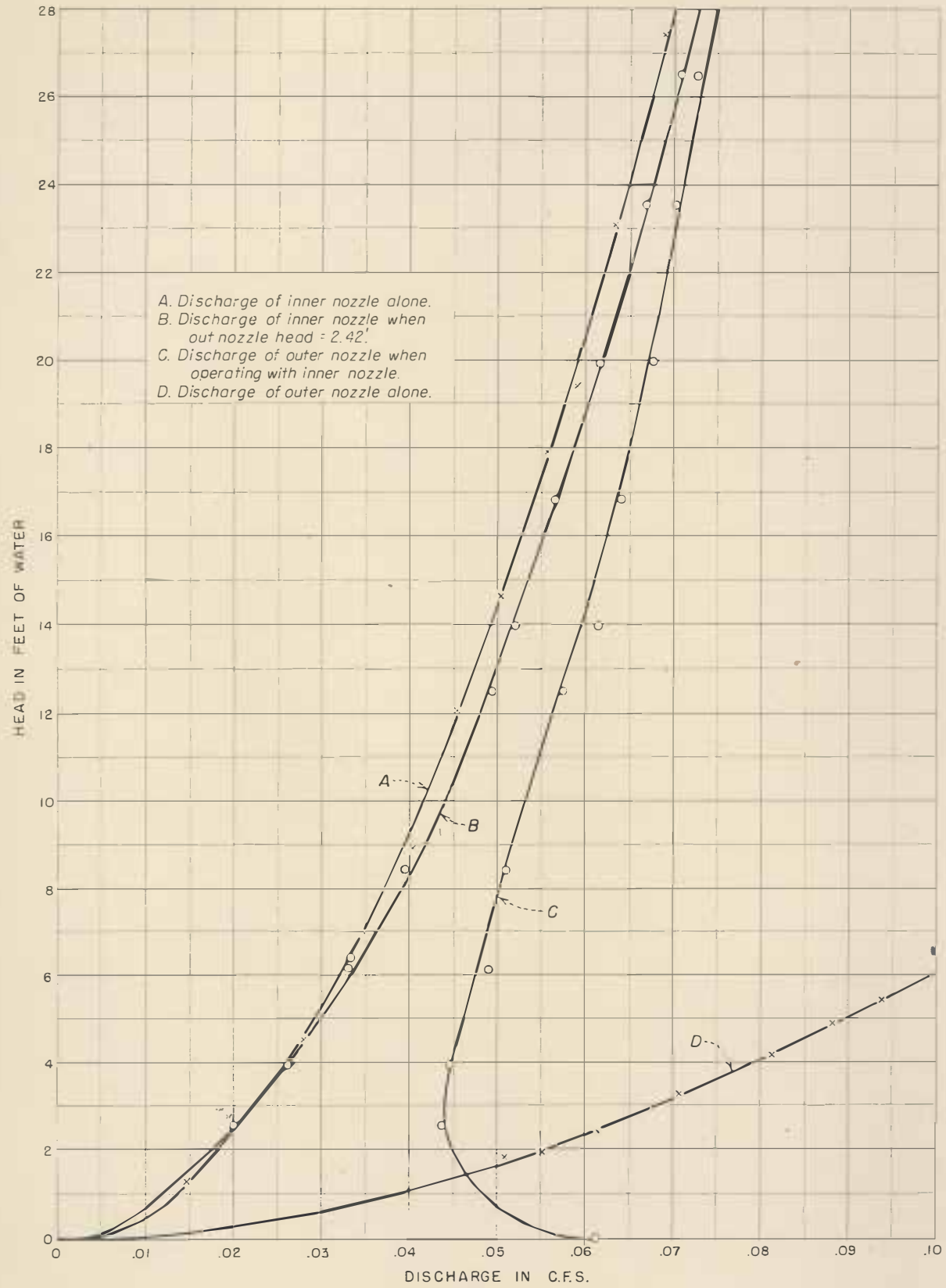

CHARACTERISTICS OF TYPE XI INNER NOZZLE

AVERAGE COEFFICIENT OF DISCHARGE = 0.79

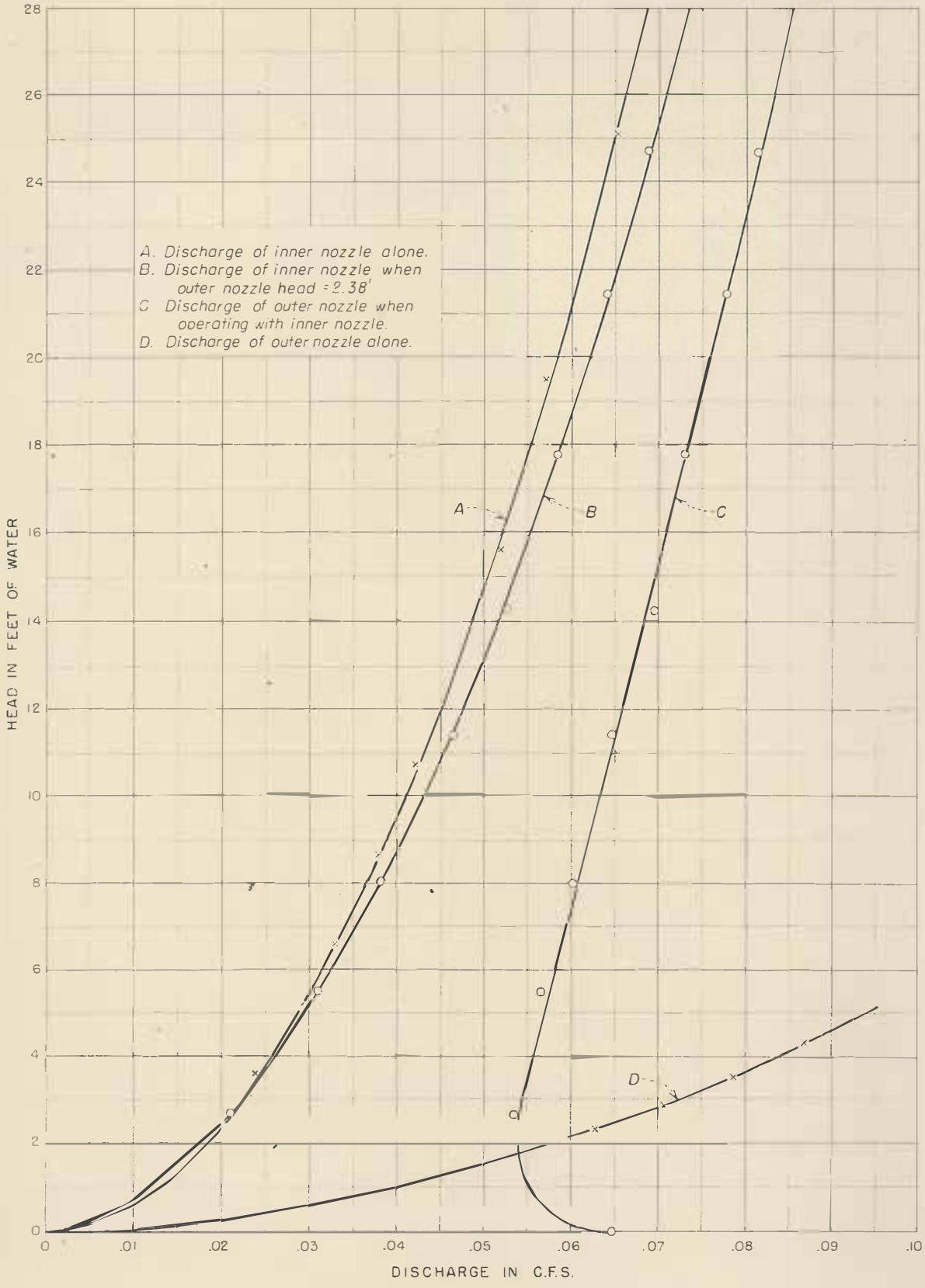

CHARACTERISTICS OF TYPE XII INNER NOZZLE

AVERAGE COEFFICIENT OF DISCHARGE = 0.95

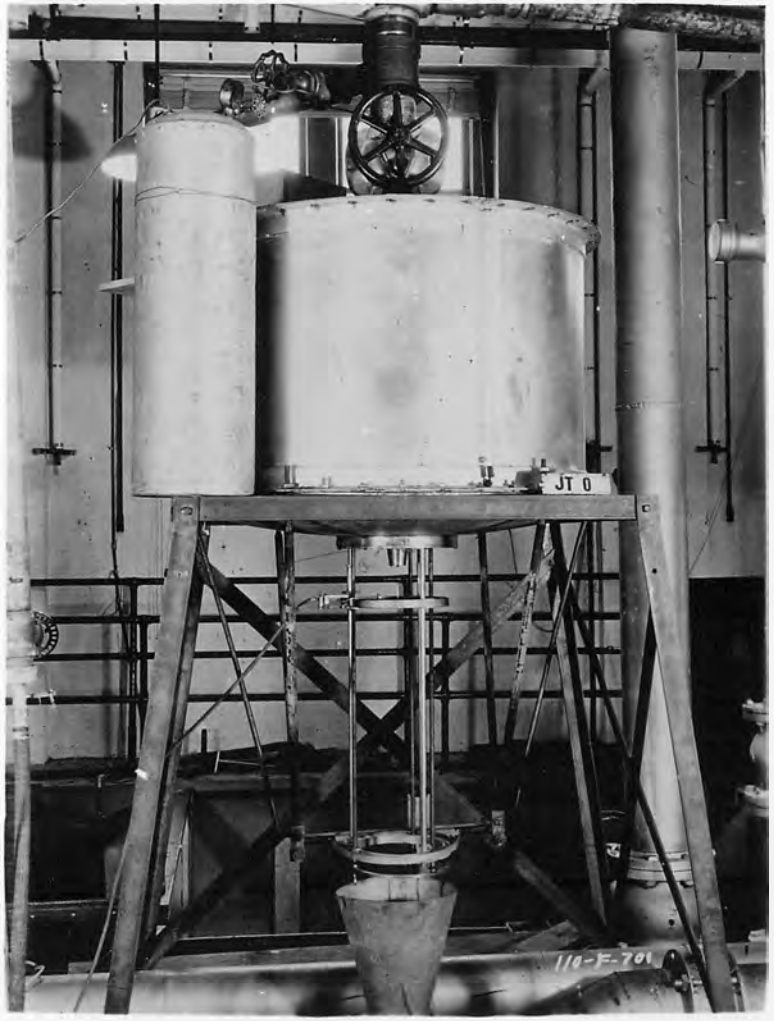

Laboratory Set-Up

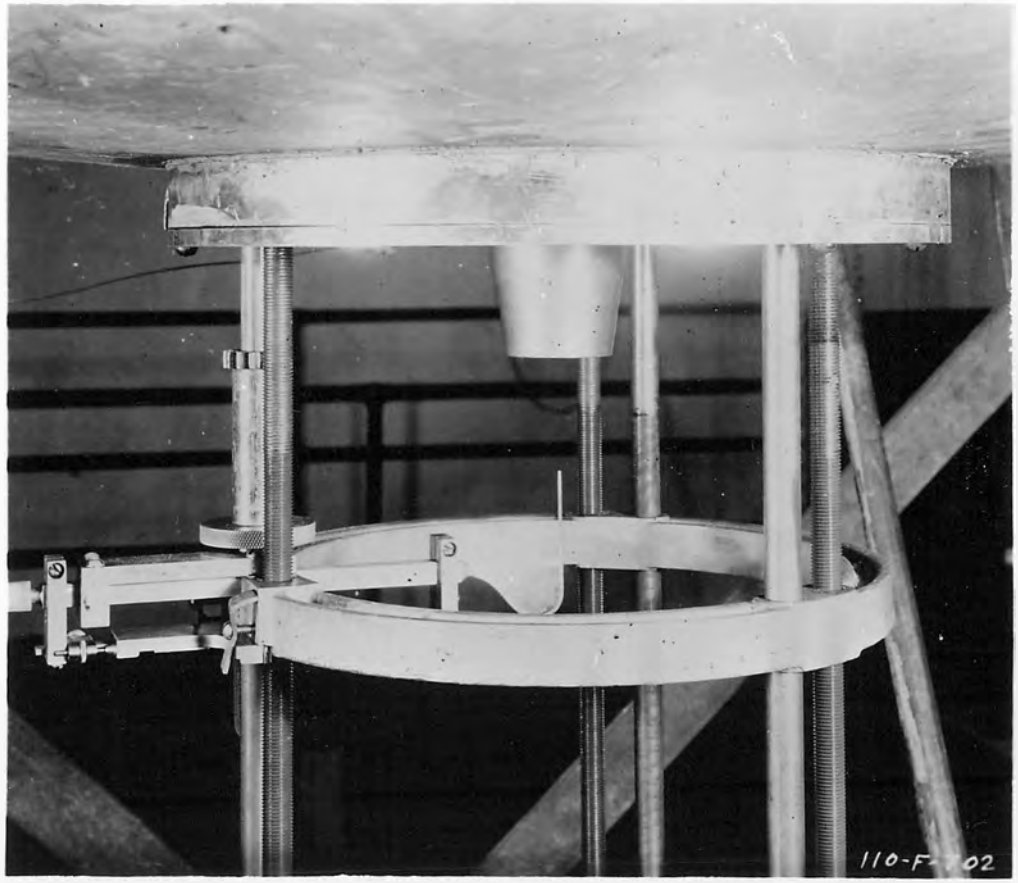

Profilometer with Pitot tube attached

PLATE I

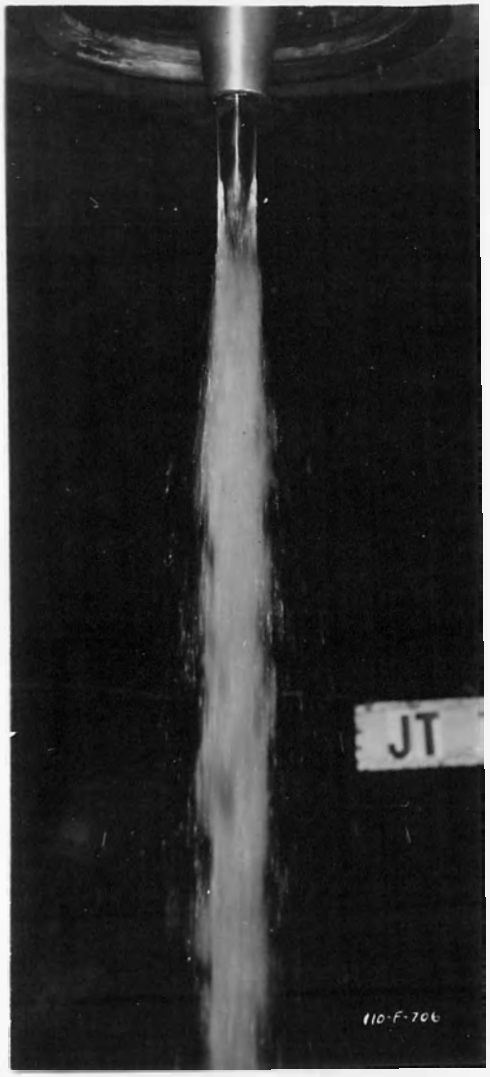

Q ratio 1:1
Inner Nozzle Q-0.0362 c.f.s.
Outer Nozzle Q-0.0362 c.f.s.

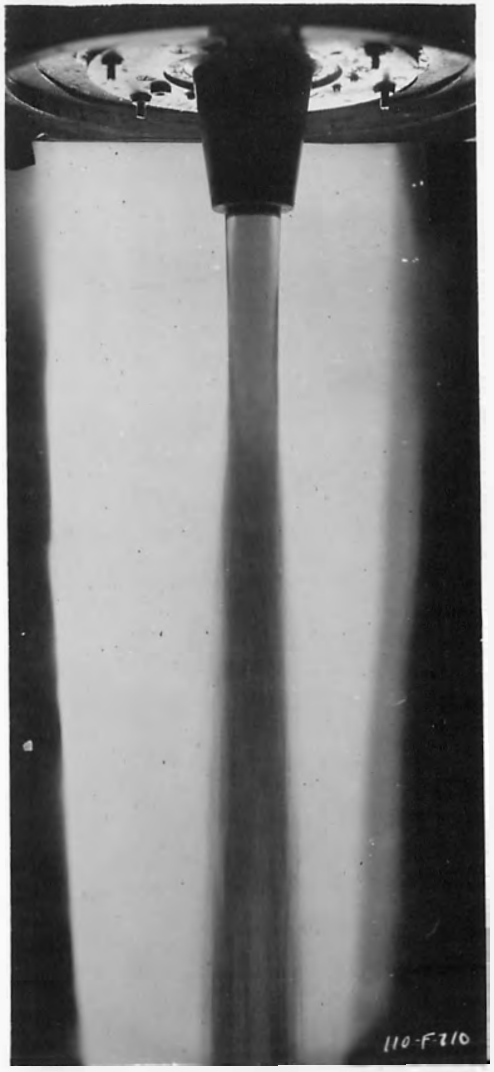

Q ratio 1:1
Inner Nozzle Q-0.036 c.f.s.
Outer Nozzle Q-0.036 c.f.s.
Dye in inner jet shows jet boundary

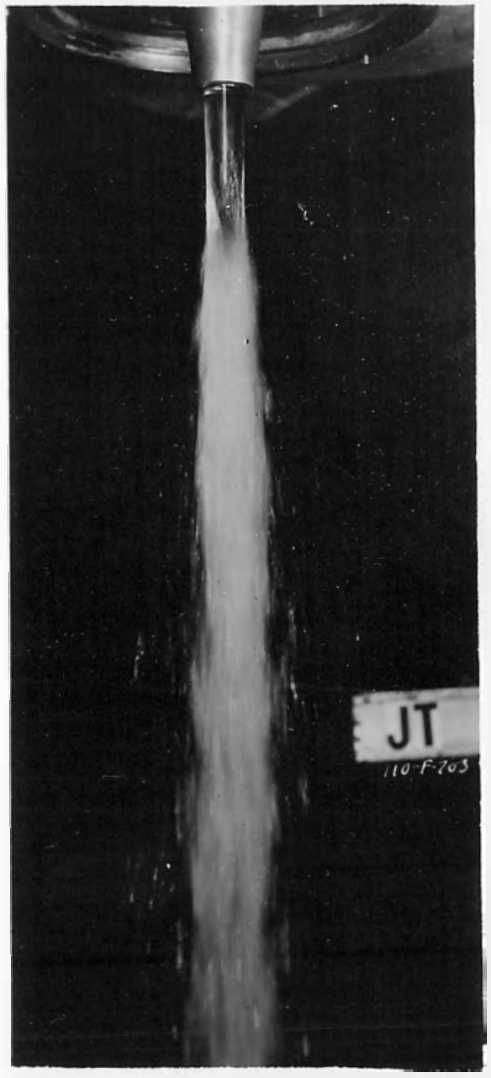

Q ratio 1:1
Inner Nozzle Q-0.0395 c.f.s.
Outer Nozzle Q-0.0395 c.f.s.

PLATE II

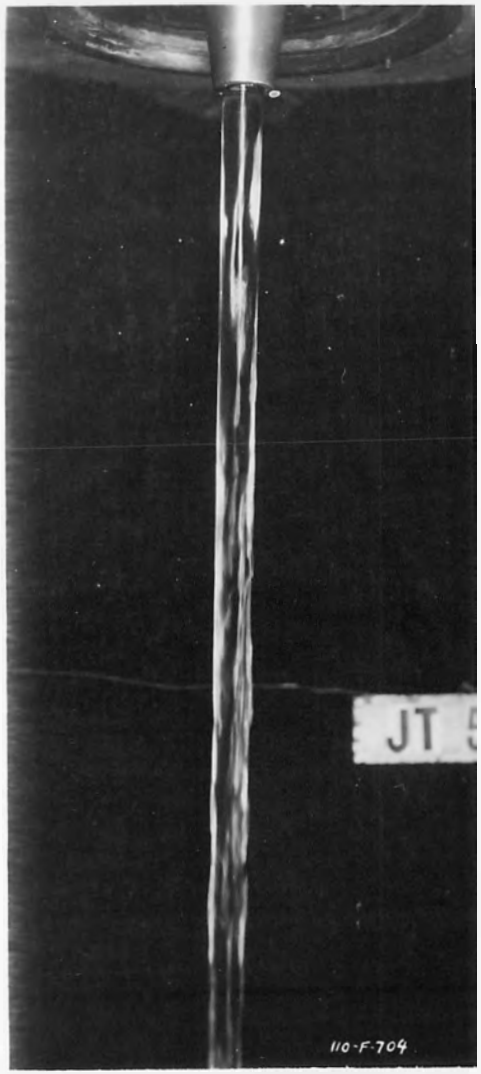

Q ratio 1/2:1
Inner Nozzle Q-0.0195 c.f.s.
Outer Nozzle Q-0.0395 c.f.s.

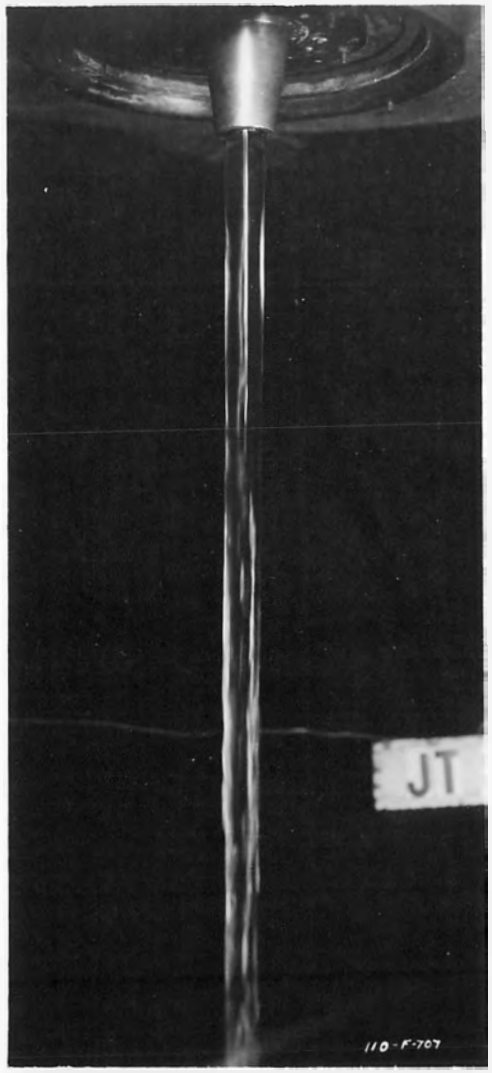

Q ratio 1/2:1
Inner Nozzle Q-0.0181 c.f.s.
Outer Nozzle Q-0.0362 c.f.s.
Dye in inner jet shows jet boundary

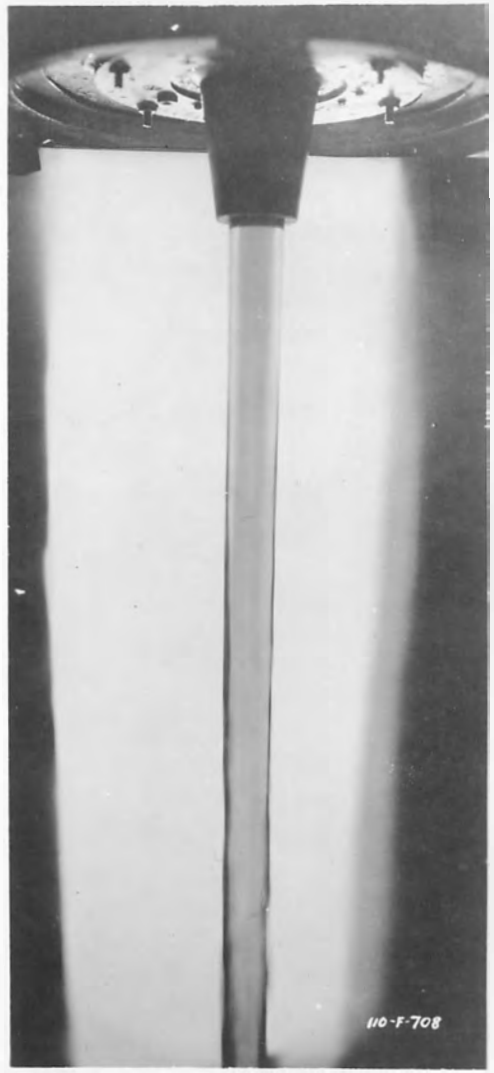

Q ratio 1/2:1
Inner Nozzle Q-0.0181
Outer Nozzle Q-0.0362 c.f.s.

PLATE III

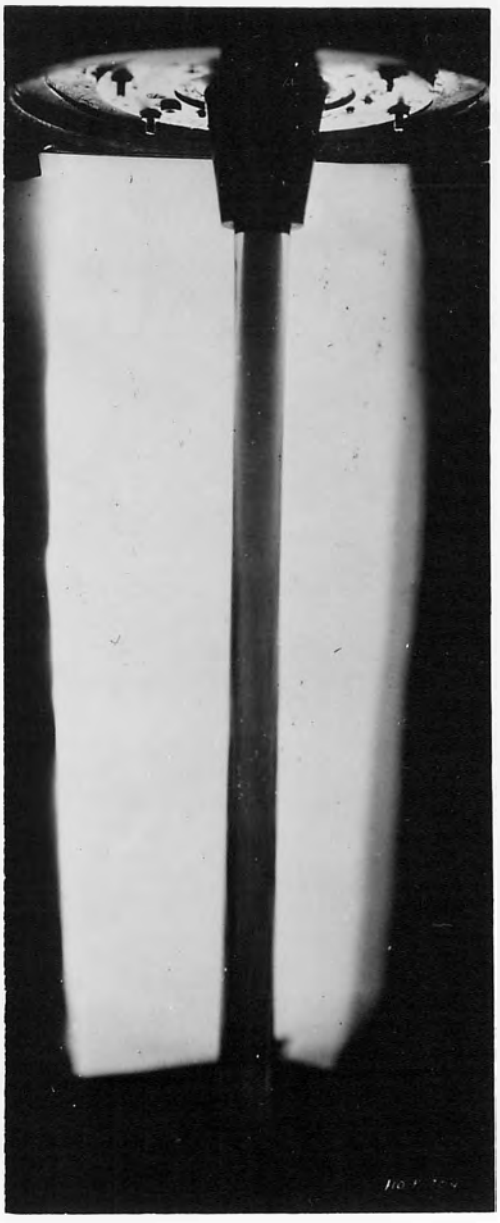

Q ratio 2/3:1
Inner Nozzle Q-0.024 c.f.s.
Outer Nozzle Q-0.036 c.f.s.
Dye in inner jet

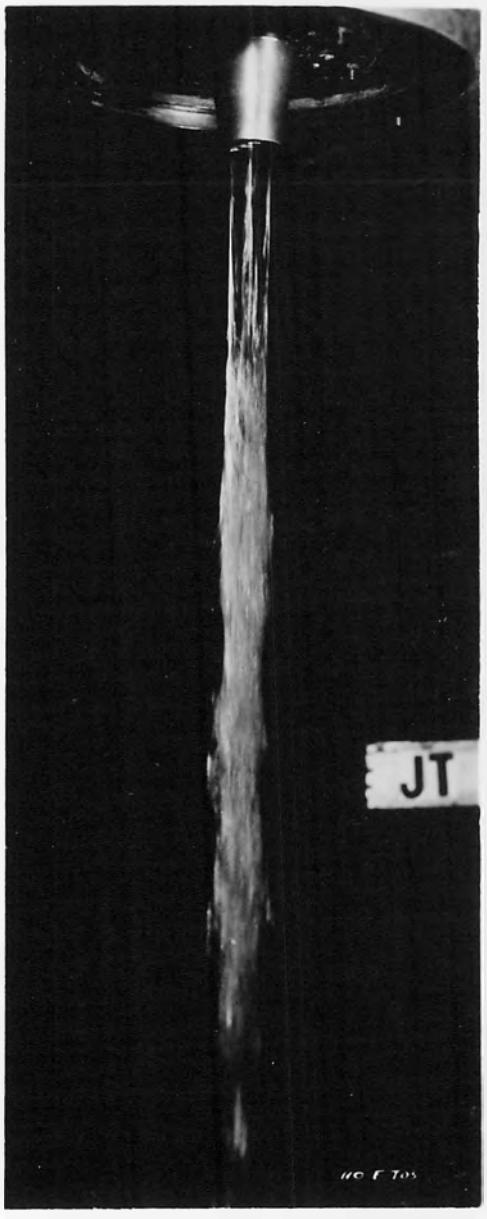

Q ratio 3/4:1
Inner Nozzle Q-0.0295 c.f.s.
Outer Nozzle Q-0.0395 c.f.s.

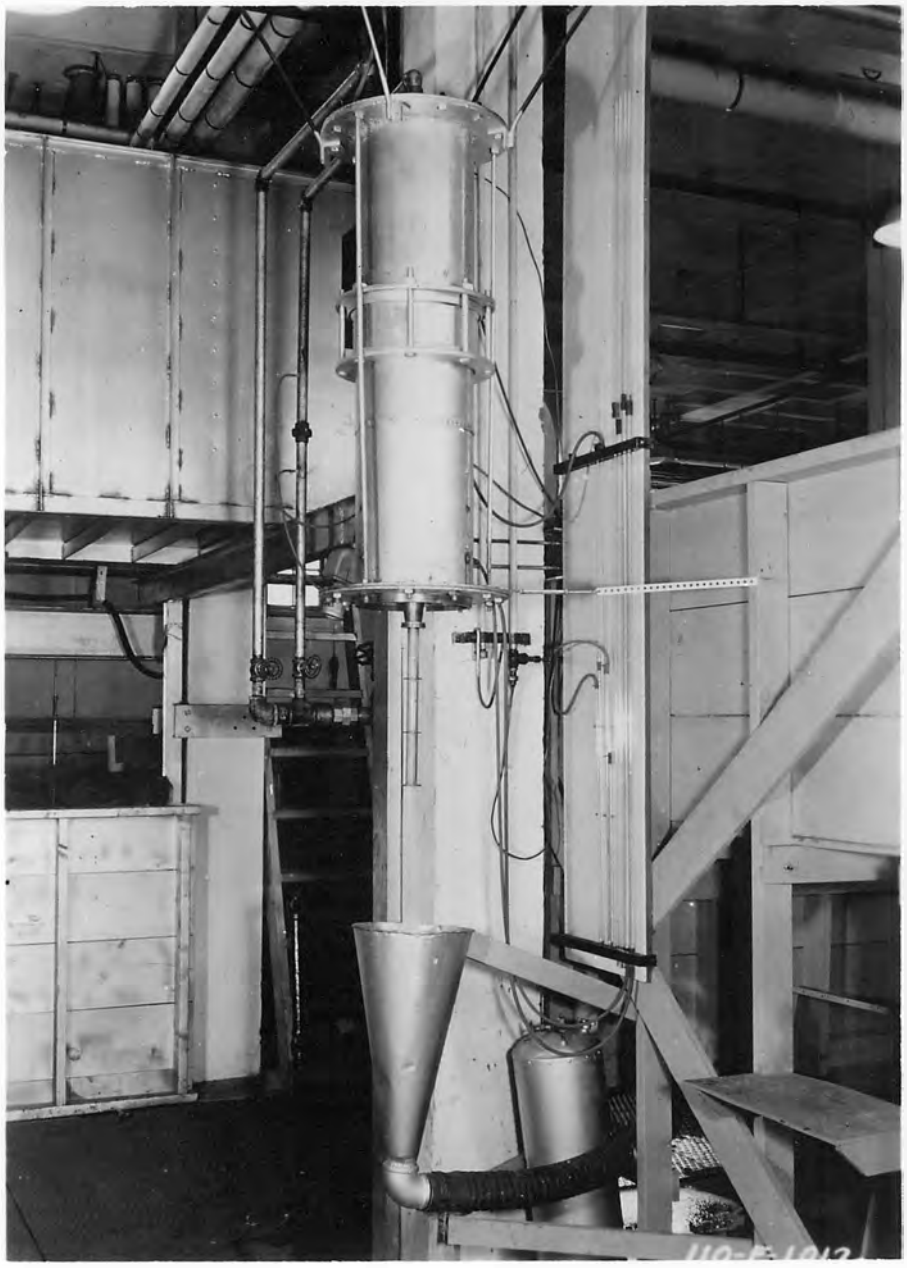

Laboratory Set-Up for Nozzle Tests

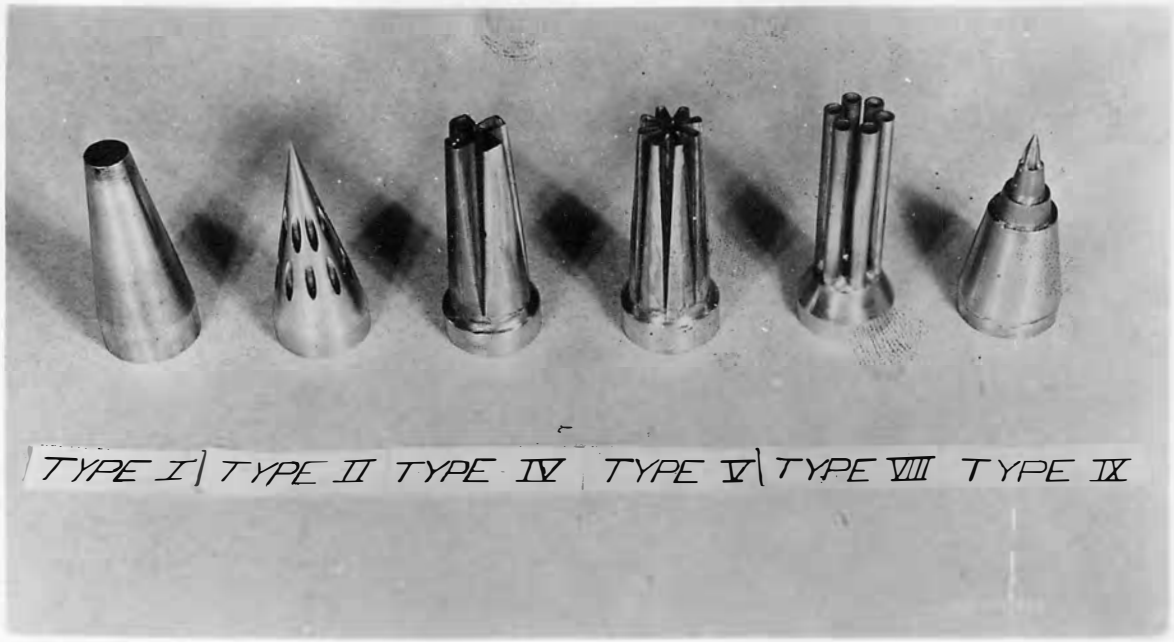

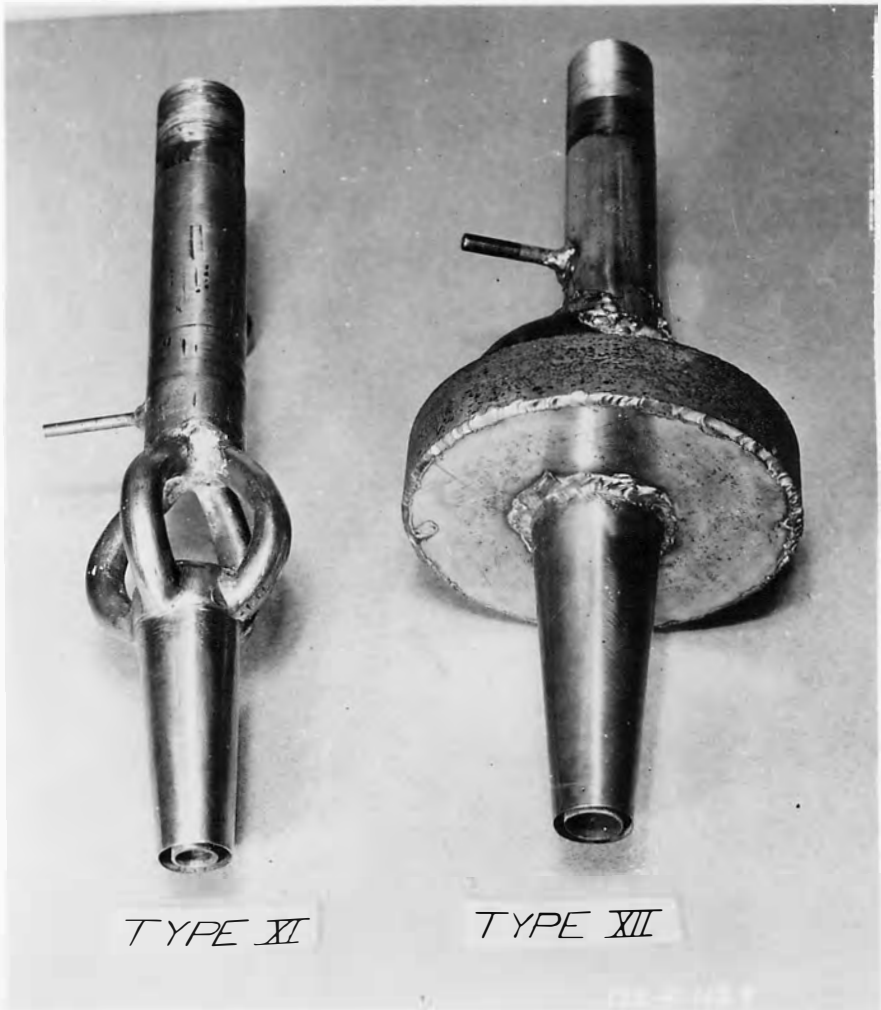

Types of Inner Nozzles Tested

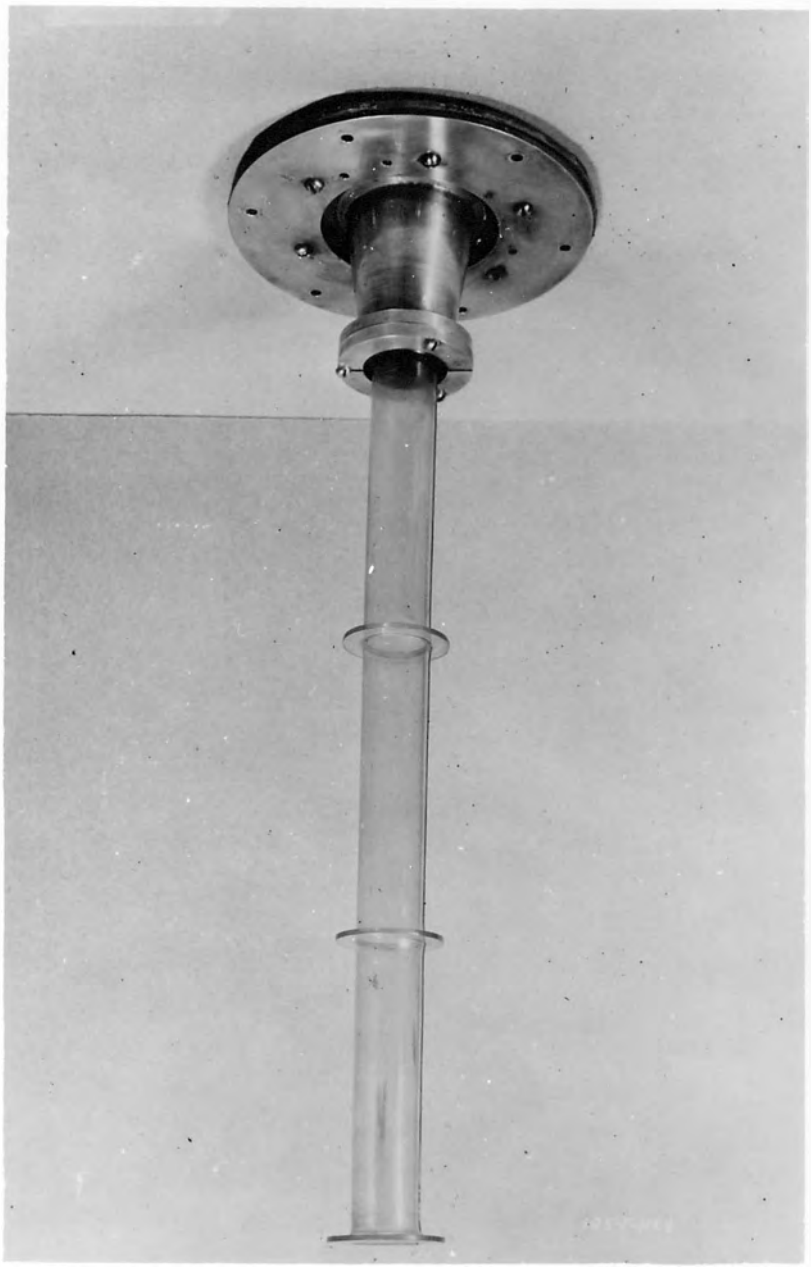

Outer Nozzle and Mixing Tube Assembly